



Identification of management options to mitigate seawater intrusion in an overexploited multi-layered coastal aquifer by integrated rainfall–runoff, surface water and density-dependent groundwater flow modeling

Sundara Pandian Rajaveni¹ · Indu Sumadevi Nair¹ · Punit Kumar Bhola² · Anna Zabel² · Bertram Monninkhoff² · Lakshmanan Elango¹

Received: 10 June 2020 / Accepted: 28 July 2021 / Published online: 3 September 2021
© The Author(s), under exclusive licence to Springer-Verlag GmbH Germany, part of Springer Nature 2021

Abstract

The objective of this research is to investigate the best management options for mitigating seawater intrusion through real-time coupling between rainfall–runoff, infiltration, surface water and groundwater system. The amount of runoff and discharge from sub-catchment after rainfall was first simulated by the rainfall–runoff model. This simulated discharge was connected with the regional surface water model to simulate the water level in the major rivers of the area. The simulated water levels in the rivers were later given as the river stage to the groundwater model through an interface module. The effect of seawater intrusion was assessed by four scenarios such as construction of additional check dams, 1 m increase in crest level of existing check dam, rejuvenation of defunct water bodies, and termination of pumping. The predicted result shows that there is an increase in the groundwater head of about 4.2 m in the unconfined aquifer and 7.5 m in the semi-confined aquifer by the end of 2030. The chloride concentration is decreased by about 1100 mg/l and 800 mg/l in the unconfined and semi-confined aquifers, respectively, by the end of 2030 with scenario 4. The areal extent has been decreased to the coast of around 5 km with scenario 4. This clearly explains that the effect of seawater intrusion is reduced by implementing mitigating measures. Finally, the real-time integrating model demonstrated that the level of groundwater is increased and the concentration of chloride decreased which helps to restore aquifer and solve the seawater intrusion problems in this study area.

Keywords Coupled model · Seawater intrusion · A–K basin · Rainfall–runoff · Density dependent

Introduction

The demand for freshwater is rapidly growing due to an increase in population, agricultural activities, and industrialization in several parts of the world. As the available groundwater resource is about 25 times greater than the surface water sources, it has been widely exploited to meet the various needs. In fact, groundwater is the world's most extracted raw material with withdrawal rates in the estimated range of 982 km³/year (Margat and Gun 2013). About 60%

of groundwater is used for agriculture; the rest is almost equally divided between the domestic and industrial sectors (Vrba and Gun 2004). As about 60% of the world's population lives on the coast, a large amount of groundwater is pumped from the coastal aquifers to meet the different human needs. Seawater intrusion caused by excessive groundwater extraction already has an impact across the globe (Ferguson and Gleeson 2012). Thus, the coastal aquifers are always under threat due to seawater intrusion and degradation of groundwater quality. Hence, optimal utilization of coastal water resources such as surface and groundwater is extremely necessary to avoid seawater intrusion.

In the hydrological processes, the connections between the surface and groundwater play an important role on the catchment scale. It is very essential to understand the interactions between the surface and groundwater flow and integrated simulation of both flows for optimal management

✉ Lakshmanan Elango
elango34@hotmail.com

¹ Department of Geology, Anna University, Chennai 600025, India

² Water Resources and Environment Department, DHI-WASY GmbH, Berlin, Germany

of surface and groundwater resources. Simulation of this coupled system by considering the interactions between the surface and groundwater is a complex process and also a challenging task. Mathematical models are effective tools to develop various models to simulate the surface and groundwater flows. Most of the models mostly concentrate on surface runoff simulation and the groundwater aspect is oversimplified (Zhang and Li 2009). Vries (1995) reported that coupling the mathematical expressions for groundwater drainage and streamflow enables the development of a conjunctive model, which relates the properties of a seasonally contracting stream network and groundwater level fluctuation. However, this coupled mathematical expression is a simplifying concept, which cannot be applicable for the complex hydrological system.

Some other models used to consider for simulating the subsurface flow, e.g., MODFLOW (McDonald and Harbaugh 1988), and river runoff, e.g., MODBRANCH (Swain and Wexler 1996). Most of the surface water models to understand the rainfall–runoff relationship consider the topographic variations (Mullem 1991; Uhlenbrook 1999; Waichler and Wigmosta 2004; Mishra et al. 2007; Anuthaman 2009; Bhadra et al. 2010; Amir et al. 2013). These models are used by these researcher's estimated groundwater recharge based on various empirical relations from the rainfall or from long-term average monthly rainfall and evaporation for assessing the impact of pumping on groundwater resources of coastal aquifers. These models have determined the interaction between the surface water and groundwater based on the temporal variation in the river stage assigned without considering the rainfall–runoff relationship. However, integrated surface water and groundwater models are necessary for analyzing complicated water resource problems, because they can consider feedback processes that affect the timing and rates of evapotranspiration, surface runoff, soil-zone flow, and groundwater interactions (Markstrom et al. 2008).

In an integrated surface and groundwater flow, one or more watersheds have simultaneously simulated the flow across the land surface, within saturated and unsaturated subsurface, and within streams and lakes (Furman 2008). The amount of surface water that infiltrates into the subsurface groundwater system depends on the rainfall rate and soil infiltration capacity (Markstrom et al. 2008). The surface–groundwater systems follow different partial differential equations. Therefore, the boundary condition is used to represent the interactions between the systems. Already existing models to develop the integrated surface and groundwater flows are SEAWAT (Langevin and Guo 2006), ParFlow code (Kollet and Maxwell 2006), DufLOW, and MicroFem (Smits and Hemker 2004), MODFLOW (Harbaugh et al. 2000), SWAT-MODFLOW (Sophocleous and Perkins 2000), TOPNET-MODFLOW (Guzha and Hardy

2010), and GSFLOW (Markstrom et al. 2008). Malamataris et al. (2019) and Kuffour et al. (2020) studied the integrated hydrological modeling of surface water and groundwater under climate change conditions. Bizhanimanzar et al. (2020) investigated surface and groundwater using conceptual and physical-based models. This integrated approach is pictorially shown in Fig. 1.

The integrated models have some advantages compared to single domain modelling, since they can represent the relationships between the surface and groundwater flows. It also has some disadvantages such as the coupled simulation may be computationally expensive and numerical instabilities may be encountered, as the governing differential equations for different flow domains must be solved simultaneously through numerical iterations (Zhang and Li 2009). Monninkhoff et al. (2011) developed a coupled surface (MIKE 11)–groundwater (FEFLOW) model used to simulate all the physical processes that are relevant to the interactions between the surface and groundwater system. The module of IfmMIKE11 is used to couple FEFLOW and MIKE11 and it has been extended for mass-transport processes. Monninkhoff and Hartnack (2011) developed a new IFM function in FEFLOW to represent the real exchange area between the river and groundwater, which mainly depends on the river profile and water depth. The new IFM function represents the exchange area by node as well as a nodal transfer rate. This function can now be optionally used in IfmMIKE11. Although many researches were carried out on the integrated surface and groundwater modeling for different aquifer systems, there was no considerable study carried out with the long-term data to assess possible management options to mitigate the seawater intrusion in the coastal aquifer system. Hence, the present study was conducted to carry out the objective of investigating the best management options for mitigating seawater intrusion through real-time coupling between rainfall–runoff, infiltration, and density-dependent catchment model using the MIKE 11 and FEFLOW packages. The reason for using the MIKE11 package was primarily because it enables direct coupling to the finite element groundwater modeling software FEFLOW using the coupling interface IfmMIKE11 (Monninkhoff 2011).

This study was carried out in an overexploited coastal aquifer, which is affected by seawater intrusion since 1969 and is situated about 45 km north of Chennai, Tamil Nadu, India. All the previous hydrological studies carried out in this study area were developed based on either the surface water model or groundwater model and they have not considered the surface water interaction through the soil and unsaturated zones to the groundwater resources. Similarly, they do not consider the effects of local geology and surface water interactions on the density-dependent groundwater model. As the region receives intensive rainfalls during short periods in monsoons, modeling of integrated surface

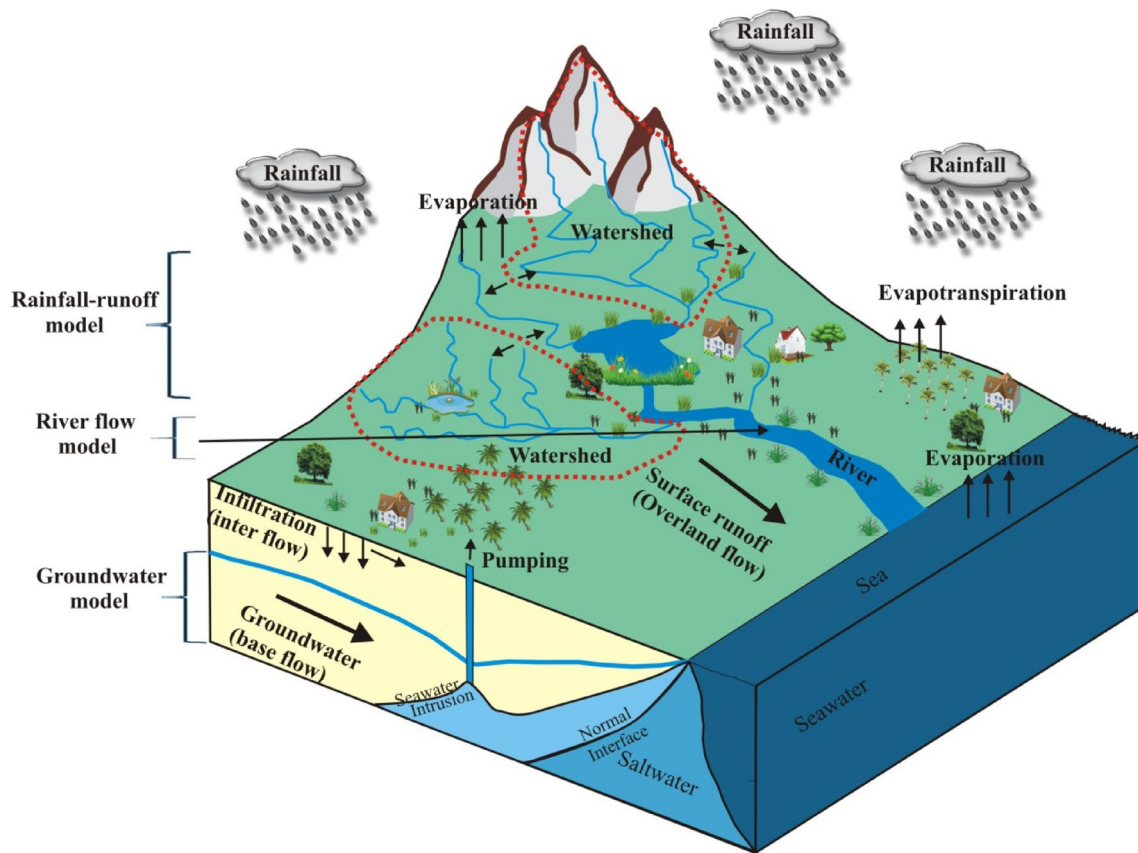


Fig. 1 Conceptualization of rainfall–runoff, river flow and groundwater model (Source: Rajaveni 2015)

water and groundwater flow is necessary to estimate the river flow, infiltration rate, and its interaction with the aquifers. It is vital to characterize the aquifer system and to assess the measures available to mitigate seawater intrusion in this aquifer. The density difference between the fresh groundwater and saline water plays an important role in the seawater intrusion studies, which is also the limitation of earlier studies carried out in the north of Chennai coastal aquifer.

Description of the study area

The study area comprises Arani and Korttalaiyar (A–K) river basin which is located north of Chennai, Tamil Nadu state, India (Fig. 2). This area experiences a very dry (summer) period from April to June with the maximum temperature ranging from 32 to 44 °C and a colder (winter) period from December to January, when the temperature ranges from 23 to 30 °C. The average annual rainfall of this area is around 1200 mm, 35% of which falls during the southwest monsoon (July–September) and 60% during the northeast monsoon (October–December). Palar River is flowing on the southwestern side of the study area. Topographically,

the area gently slopes toward the east. A–K rivers are non-perennial and join the Bay of Bengal in the east. Both rivers generally flow only for a few days during the northeast monsoon (October–December) period. However, the river generally has saline backwaters during the rest of the time up to 5 km from the sea. Buckingham canal, a manmade canal, runs parallel to the coast was constructed for navigation purposes during the nineteenth century, which always carries saline water as it is connected to the sea at a number of places. The total surface area of the A–K basin is about 6225 km², of which about 1456 km² is covered by alluvium and buried paleo river channels (UNDP 1987) of the Palar River. This area was considered for the purpose of groundwater modeling (Fig. 2). The boundary of the study area in the north, south, and west side was fixed where the thickness of the alluvium is less than 10 m. Agriculture is the major activity and the main crops cultivated in this area are rice, pulses, groundnut, sesame, sugarcane, and vegetables.

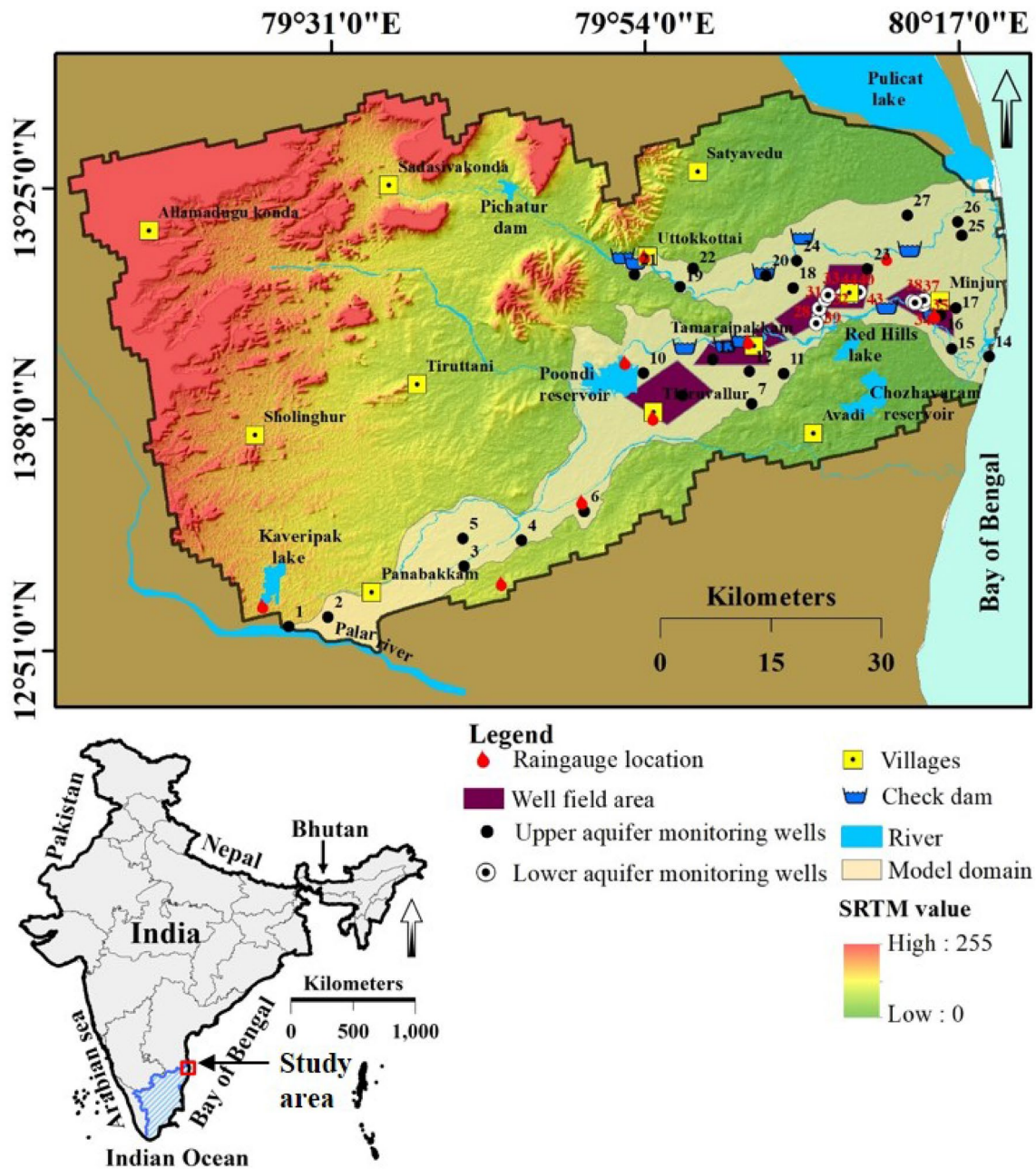


Fig. 2 Location of Arani–Korttalaiyar (A–K) river basin in India

Geology

Geologically, this area comprises rocks from Archaean to Quaternary age. The stratigraphic sequence of the area is given in Table 1. Crystalline rocks of Archaean age comprising gneiss and charnockite form the basement. The upper Gondwana series of shale and clay deposits lie over these crystalline rocks. Tertiary and Quaternary deposits lie over the Upper Gondwana formation of a massive pile of lacustrine and fluvial deposits (Rao et al. 2004). A thick pile of Gondwana shales and clays below the recent

Table 1 Geological succession of the study area (Data source: based on UNDP 1987)

Quaternary	Alluvium, fine to coarse sand, gravel, laterite, silty sand, clay and clayey sand
Tertiary	Shale, clay and sandstone
Upper Gondwana	Gondwana shale and clay
Archaean	Crystalline rocks, charnockite and gneiss

alluvial deposits (Rao et al. 2004) underlie the central and eastern parts. The geological map of the area obtained from the Geological Survey of India (GSI) in 1:50,000 scale was updated by interpreting the Indian Remote Sensing Satellite's Linear Imaging Self Scanning sensor system (IRS 1D LISS-III) imagery, which is of 23.5 m spatial resolution. The geological map thus prepared was validated through field visits and it is shown in Fig. 3. The northwest part of the area

is covered by sandstone with calcareous gritstone, sandstone and conglomerate. The Quaternary deposit consists of laterite and alluvium. The area considered for modeling consists of alluvial deposits comprising sand and silt, sandy clay, gravel, and pebbles that mostly occur along with the A–K river courses. Sand is the dominant fraction in alluvial and aeolian deposits near the coast.

Hydrogeology

The alluvial deposits are characterized by a number of clay lenses and thus the deposit is divided into two water-bearing layers up to a distance of 30 km toward west from the coast by a clay layer of about 3–5 m thickness, which functions as an aquitard. The geological cross section was prepared based on the lithology collected from Chennai Metro Water Supply and Sewerage Board (CMWSSB) as shown in Fig. 4. The dug wells are generally less than 20 m deep and tube wells are up to 120 m deep. The type and number of aquifer system are assessed based on the lithology, field investigations, and measurement of groundwater head. The presence of two aquifer systems consisting of the unconfined and semi-confined aquifer was identified until 30 km from the coast, and beyond this distance, the two aquifers merge and become a single aquifer (Fig. 4). The groundwater head

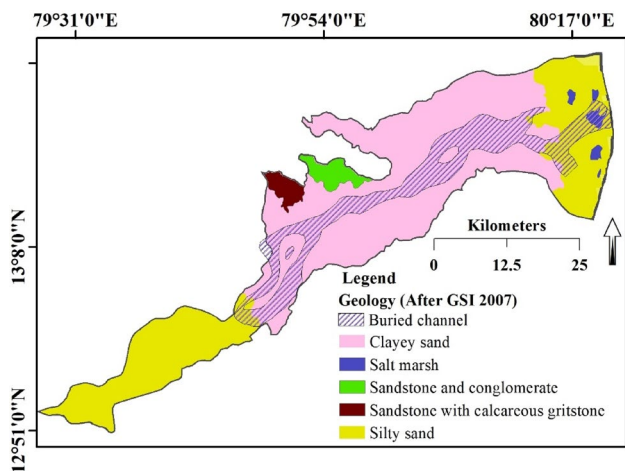


Fig. 3 Geology of the area considered for groundwater modeling

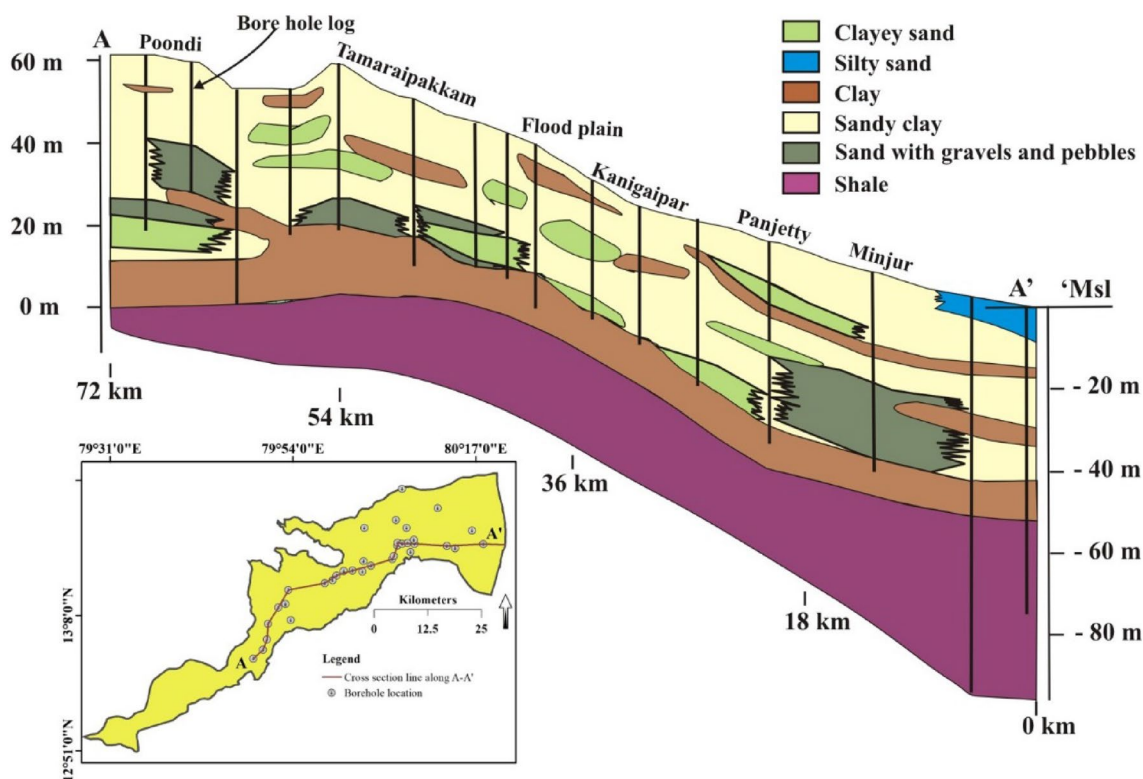


Fig. 4 West to east geological cross section along A–A' (top right) of the area considered for groundwater modeling

in the unconfined aquifer ranges from 2 to 6 m bgl (below ground level), and in the semi-confined aquifer, it ranges from 14 to 20 m bgl. Rao et al. (2004) and Charalambous and Garratt (2009) studied the recharge and abstraction relationship through the finite element model for this region only by considering it as a single confined aquifer system. In general, the regional groundwater flow is toward the sea; however, there may be variations in local hydraulic heads due to the difference in the pumping pattern. The water from these wells is used for domestic, irrigational, and municipal purposes. Six well fields were located in the alluvial deposits, paleo buried channels (Suganthi et al. 2013), and the groundwater is being pumped from 98 wells to meet a part of the Chennai City's water requirement. The hydraulic conductivity of the upper unconfined aquifer varies from 35 to 100 m/day (Rajaveni 2016). Hydraulic conductivity of the semi-confined aquifer varies from 120 to 250 m/day (Rajaveni 2016). The hydraulic conductivity and the thickness of the semi-confined aquifer are comparatively higher than those of the unconfined aquifer and, hence, the semi-confined aquifer is the major aquifer near the coast. Due to the interaction between the unconfined and semi-confined aquifer during pumping, it is crucial to consider both aquifers for modeling. As the region receives intensive rainfall during short periods during monsoons, modeling of coupled surface water and groundwater flow is necessary to estimate the river flow, infiltration rate, and their effect on the aquifers.

Groundwater recharge and pumping

The sources of groundwater recharge are rainfall, riverbed infiltration, and irrigation return flow. Out of these three sources, rainfall infiltration is the major source for

groundwater recharge. The rainfall infiltration method was used to calculate monthly recharge as recommended by the Groundwater Resources Estimation Committee (GEC 1997). GEC (1997) suggested the use of rainfall infiltration factor for different geological conditions, to estimate the groundwater recharge in the study area. There are nine rain gauge stations located in the study area (Fig. 2) that were also considered for calculating groundwater recharge. Based on the geology and the location of the rain gauge stations, the area was divided into nine Thiessen polygons to define monthly groundwater recharge (Fig. 5a). Based on Charalambous and Garratt (2009), geology and GEC (1997) norms, the groundwater recharge was assigned from 10 to 20%. River water level calculated from MIKE 11 HD was assigned to river boundary nodes by coupled IFM module. In addition, the return flow from the agricultural field aids in groundwater recharge. Previous studies carried out in the A–K basin by Charalambous and Garratt (2009) and Anuthaman (2009) stated that almost 39% of irrigation water returns to the aquifer in this area. Hence, 39% of pumped water was considered as irrigation return flow.

Groundwater in the area is the major source for irrigation, domestic, and Chennai City's municipal water supply. Groundwater pumping rate for irrigation can be calculated by three different methods such as electricity consumption, the horsepower of pumps used, and crop water requirement. But in Tamil Nadu, it is very difficult to calculate groundwater pumping from the electricity consumption and pump type, because electricity is distributed free of cost by the government for extracting groundwater for irrigation purpose. Hence, groundwater pumped for irrigation was estimated based on the crop water requirement. The type of crops grown during different seasons was mapped for a year by using satellite remote sensing data (Rajaveni et al. 2014). Land use pattern was prepared from IRS 1D LISS-II

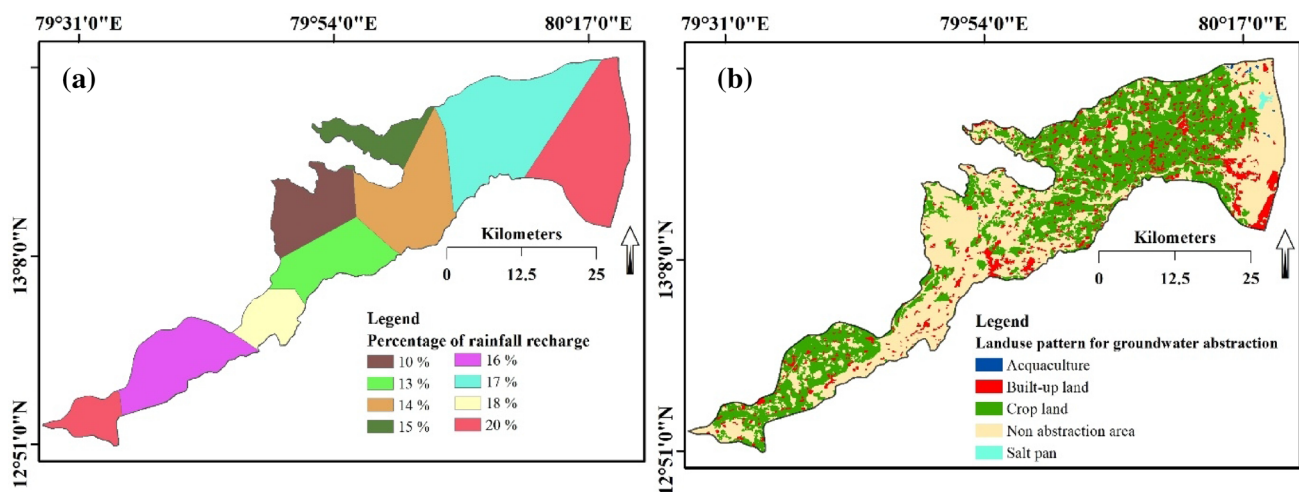


Fig. 5 **a** Percentage of groundwater recharge and **b** land use pattern for estimation of pumping used for groundwater modeling

imagery (Fig. 5b). The area was classified into 12 land use categories such as paddy, plantation, other crops, permanent fallow, current fallow, residential, wasteland, water bodies, wetlands, forest, salt pan and aquaculture. Groundwater pumping rate for various purposes such as domestic, salt pan and aquaculture were estimated based on the per capita demand, a number of pumps with horsepower used, and water replacing days, respectively. For domestic pumping, per capita demand required for town Panchayat was taken from Tamil Nadu Water Supply Board; the per capita demand of groundwater of this area is 0.07 m³/day. The estimated groundwater pumping was about 480 Mm³/year. In addition to irrigation pumping, groundwater is also continuously pumped from the well fields for the Chennai municipal water supply. The pumping rate from the six-well fields was collected from CMWSSB, namely Minjur, Panjetty, Kanigaipar, Tamaraipakkam, Flood plain and Poondi for a year.

Methodology and model setup

The brief description of the integrated model concept used in the present study is shown in Fig. 6. The methods and tools used to generate the catchment scale model are as follows:

1. A rainfall–runoff model (NAM) to produce surface water inflow at the sub-catchment scale for the boundary conditions into the surface water system as well as the infiltration into the subsoil, integrated in the 1D surface water model.
2. A one-dimensional surface water model (MIKE 11) for the two rivers, Arani and Korttalaiyar.
3. A three-dimensional groundwater model (FEFLOW) for the alluvial aquifers of A–K basin, which is coupled to the MIKE 11 model using the coupling interface Ifm-MIKE1.

Rainfall–runoff model (NAM)

The Nedbør–Afstrømnings model (NAM), meaning precipitation–runoff mode model, operates by continuously accounting for the moisture content in four different and mutually interrelated storages that represent overland flow, interflow, base flow, and precipitation. As NAM is a lumped model, it treats each sub-catchment as one unit; therefore, the parameters and variables considered represent average values for the entire sub-catchments. Figure 7 displays the concept of the NAM model. The NAM model includes nine basic parameters to generate runoff from given rainfall and evaporation. The basic parameters used for the

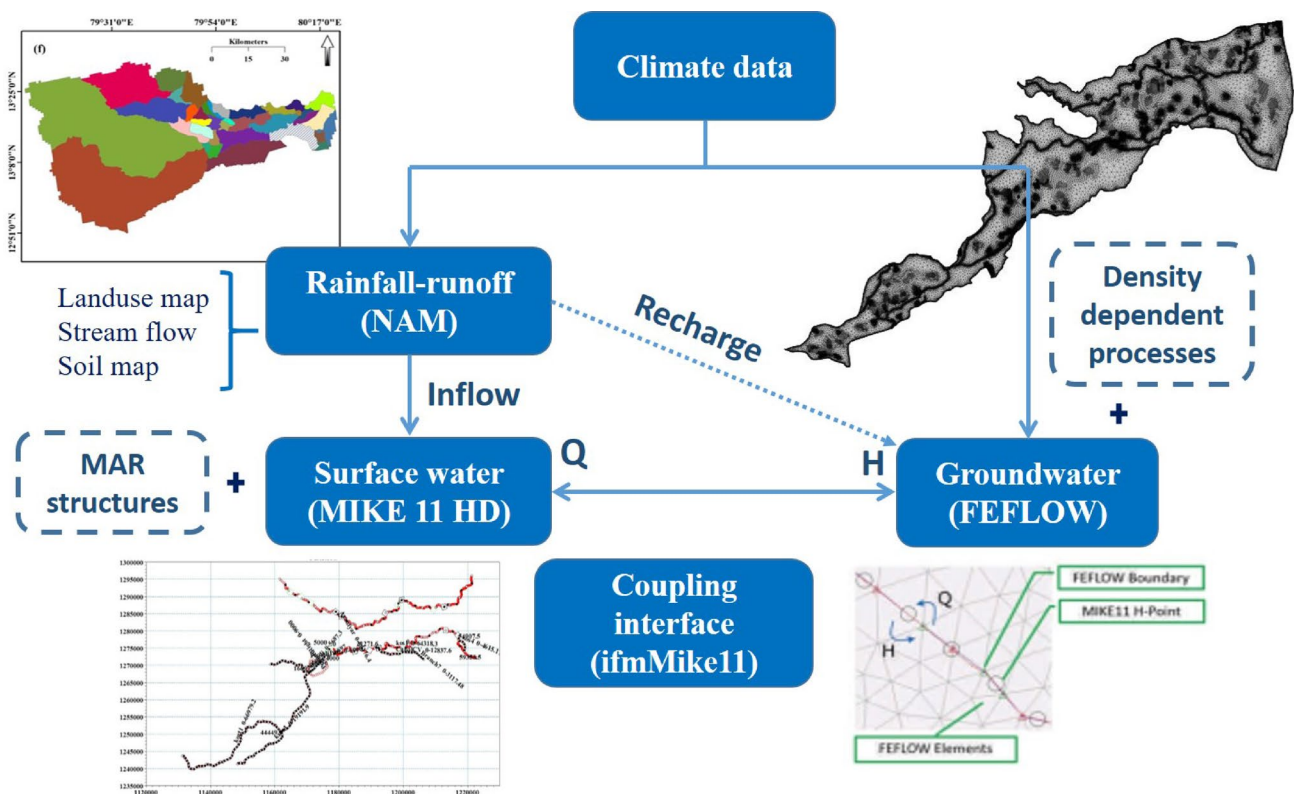


Fig. 6 Brief description of the integrated model concept

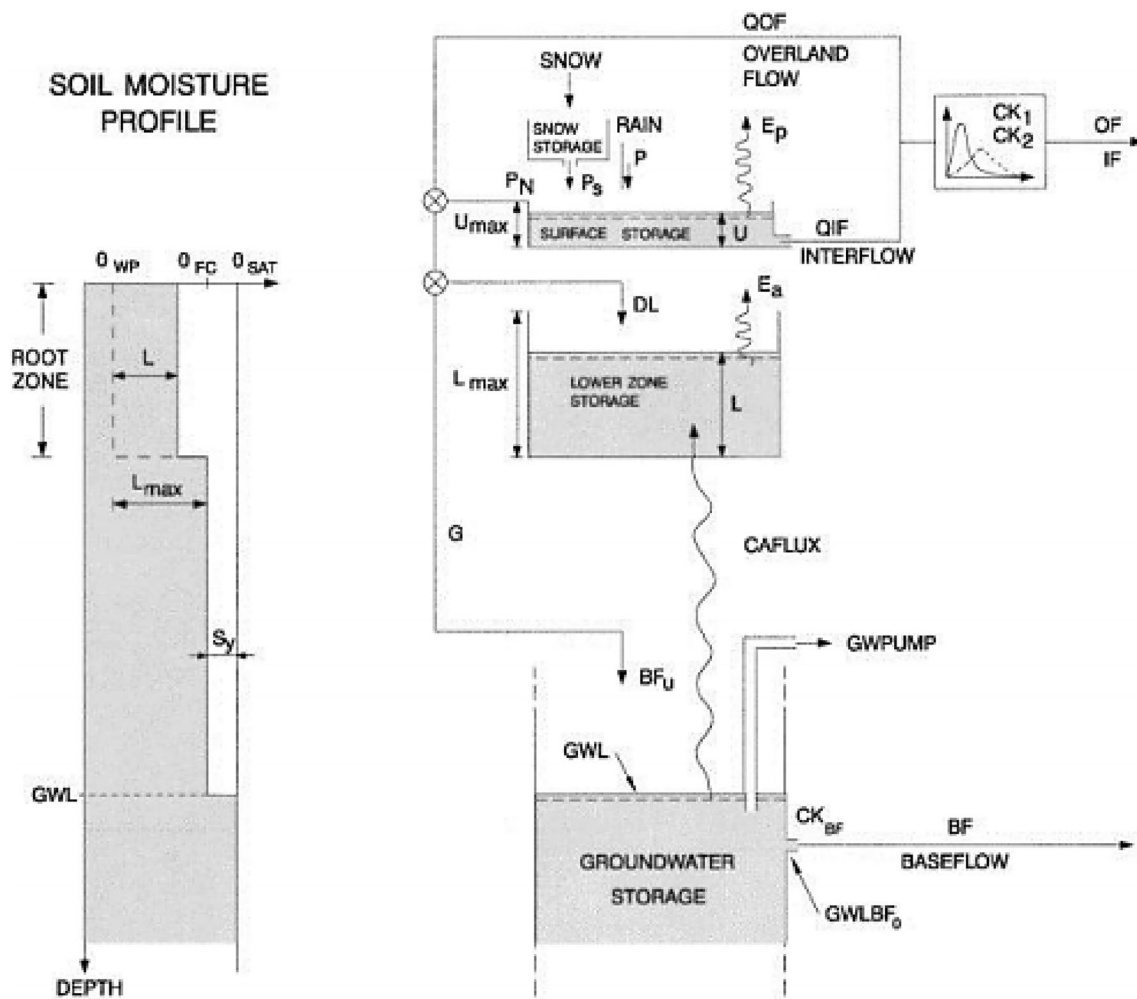


Fig. 7 Basic structure of the NAM model concept (DHI 2007)

rainfall–runoff model (DHI 2017) are: (1) maximum water content in surface storage (U_{max}), which is an important parameter and plays an important role in altering the values of the overland flow, recharge, amount of evapotranspiration, and intermediate flow; (2) the maximum water content in the root zone storage (L_{max}) can be estimated by subtracting the field capacity and wilting point, which is multiplied by effective root depth; (3) overland flow runoff coefficient (CQOF), which is a very important parameter and describes the fraction of excess rainfall that generates overland flow and magnitude of infiltration; physically, in a lumped manner, it reflects the infiltration and also to some extent the recharge conditions; it is a dimensionless factor between 0.01 and 0.99; (4) time constant for interflow (CKIF) determines the rate at which surface water (U) drains into interflow storage and its values are in the range 500–1000 h; (5) time constant for routing interflow and overland flow ($CK_{1,2}$) determines the shape of the hydrograph for the overland flow and interflow components; its value depends on the size of

the catchment and how fast it responds to rainfall; typical values are in the range 3–48 h.; (6) for root zone threshold value for overland flow (TOF), the maximum value of 0.99 is allowed as threshold; (7) root zone threshold value for interflow (TIF); (8) base flow time constant (CKBF); and (9) root zone threshold value for groundwater recharge (TG), which determines the relative value of the moisture content in the root zone, above which groundwater recharge is generated and assigned the maximum value of 0.99.

Apart from these nine surface water parameters, few groundwater elements were also used. Groundwater elements include the ratio of the areal catchment of groundwater to surface water catchment (C_{area}), the specific yield for the groundwater storage (S_y), maximum groundwater depth causing base flow, seasonal variation of maximum depth, depth for unit capillary flux, groundwater pumping, lower base flow and time constant for routing lower base flow. The values of all these parameters for the NAM model cannot be

obtained directly from measurable quantities of catchment characteristics (Hafezparast et al. 2013).

Surface water model (MIKE 11 HD)

Surface water modeling was performed by the MIKE11 hydrodynamic (HD) module. The HD module uses an implicit, finite difference scheme for the computation of unsteady flows in rivers and estuaries (DHI 2005). MIKE 11HD, when using the fully dynamic wave description, solves the equations of conservation of continuity and momentum:

$$\frac{\partial Q}{\partial x} + \frac{\partial A}{\partial t} = q, \quad (1)$$

$$\frac{\partial Q}{\partial t} + \frac{\partial \left(\alpha \frac{Q^2}{A} \right)}{\partial x} + gA \frac{\partial h}{\partial x} + \frac{gQ|Q|}{C^2AR} = 0, \quad (2)$$

where Q is the discharge, A the flow area, q the lateral flow, h the stage above datum, C the Chezy resistance coefficient, R the hydraulic or resistance radius, and α the momentum distribution coefficient.

The rainfall–runoff model (NAM) forms part of the MIKE 11 River modeling system for simulation of the rainfall–runoff process in sub-catchments (Havnø et al. 1995). The sub-catchment from the rainfall–runoff model is linked to the corresponding river network point and real-time coupling between surface water model and rainfall–runoff model was attained. The outputs such as runoff, overland flow, and infiltration obtained from the NAM model were linked to MIKE 11 by assigning the boundary conditions in the MIKE 11-HD model. Boundary conditions are assigned as inflow hydrographs derived at daily time steps from the rainfall–runoff model (NAM) on all upstream boundaries and seawater levels at the downstream end. The open boundary condition has been specified at free upstream and downstream ends with a daily time series of the inflow and constant water level downstream.

The simulation was carried out from the year 2004, and eight check dams of 1.5 m height that were present at the time across these rivers were also considered. These rivers are discretized into the number of nodes of size from 100 to 400 m. These nodes were later connected to the river boundary nodes of the groundwater model. In MIKE 11 HD, the river cross-sectional profiles were generated for every 5 km from Google Earth and a topographic survey was also conducted using a Leica TS06 model at six locations in the river channels. The A–K river network was considered on the basis of river cross-sectional data.

Groundwater model (FEFLOW)

The detailed hydrogeological study was carried out in the A–K basin to demarcate the boundary for groundwater modeling. A drainage map was derived from Space Shuttle Terrain Mapping (SRTM) and Survey of India toposheet. The Geological Survey of India (GSI) map is used to prepare the geology map. Borehole logs collected from Chennai Metropolitan Water Supply and Sewerage Board (CMWSSB) were used to prepare subsurface lithology. The model boundary was demarcated by considering drainage, geology, and subsurface formations. The groundwater model of the area was created in three dimensions using Finite Element subsurface FLOW (FEFLOW) 6.2 version software. The model area of 1456 km² was discretized into finite element mesh, consisting of approximately 1.5 million triangular elements. These triangular elements were further refined along the river course and around the well fields for simulating the groundwater head and the solute transport with greater accuracy. Thus, the length of a finite element cell varies between 30 m (near well field and river) and 1000 m in other areas. The alluvial formation was considered as eight independent layers for modeling based on the lithological variations observed in the area.

The eastern side of the study area is bounded by the Bay of Bengal and is implemented as the constant head boundary. The northern and southern boundaries are watershed boundaries. The groundwater flow from these boundaries is negligible and they are considered as the no-flow boundary. The Palar River flows in the southwestern boundary and the A–K rivers cross the western boundary, which is considered as the time-varying head boundary. The time-varying head was assigned based on the groundwater head observed in the nearby wells (Fig. 2). The nodes along the A–K rivers were defined as a fluid-transfer boundary condition for coupling with MIKE 11 HD. As the groundwater head of January 1996 was more an average head measured between the years 1995 and 1997, this period was selected as the initial head. Groundwater head from the year 1995 to 2013 for 27 monitoring wells in the unconfined and 13 monitoring wells in the semi-confined aquifers was collected from Tamil Nadu Public Works Department and CMWSSB, respectively. The aquifer properties such as hydraulic conductivity and specific yield were obtained from a pumping test conducted by UNDP (1987).

Coupling concept

The groundwater model needs to consider the recharge from the two major rivers flowing in the study area. For this purpose, the nodes in the rivers were considered as fluid transfer boundary. The river water level estimated by MIKE 11-HD based on the river discharge, generated by considering the

input from the various sub-catchments (NAM model), was assigned at the fluid transfer boundary. That is, the river water level simulated by MIKE11-HD at the end of the previous time step was used to define the actual boundary values at the nodes in the rivers of the FEFLOW model. In FEFLOW, a river described by fluid transfer boundary type is the only type supported by the coupling module IfmMIKE11. At the end of each FEFLOW time step, the exchange rates to these FEFLOW boundary nodes are calculated by the module within FEFLOW. The time step of the groundwater model is controlled by FEFLOW. The spatial overlay of both meshes is automatically integrated within IfmMIKE11 (Monninkhoff and Hartnack 2011). The nodal exchange of discharge (Q) between the ground and surface water is calculated within FEFLOW separately for each single fluid transfer boundary node. The main parameter to control this discharge is an elemental parameter called transfer coefficient \varnothing_h (Monninkhoff 2011):

$$Q = \varnothing_h A (h_{\text{ref}} - h_{\text{gw}}), \quad (3)$$

where Q is the discharge of the fluid (m^3/day), \varnothing_h is the transfer rate or leakage factor (day^{-1}), A is the nodal representative exchange area of the boundary node (m^2) and h_{ref} and h_{gw} are heads in the river and groundwater (m), respectively.

The resulting discharge values calculated from FEFLOW were transferred to the coupled MIKE 11 HD H points as an additional boundary condition (Q -base). MIKE 11 HD calculates as many as internal time steps needed to reach the actual time of FEFLOW. The internal time step of MIKE11 HD can be set in the ifmMIKE11 module. After this has been done, the actual water level of the MIKE11 HD H points was exported to the FEFLOW coupling boundary nodes and FEFLOW starts its next time step (Monninkhoff 2011). Further, the MIKE 11-HD will also have considered the inflow if any generated by the NAM model. The groundwater head simulated by FEFLOW is again given as an input for the NAM model to generate the overland and base flow going out of the sub-catchment.

Density-dependent seawater intrusion model

Three-dimensional density-dependent mass transport is modeled in FEFLOW on the basis of Darcy law and non-linear (non-Fickian) dispersion law (DHI 2009). In the linear Fickian law, the dispersive mass flux of a solute is proportional to the solute concentration gradient. Divergence (4) and convergence (5) form of transport equation using FEFLOW (DHI 2009) is given below:

$$\frac{\partial}{\partial t}(RC) + \frac{\partial}{\partial x_i} \left(q_i^f C - D_{ij} \frac{\partial C}{\partial x_j} \right) + R\vartheta C = Q_C, \quad (4)$$

$$R_d \frac{\partial C}{\partial t} + q_i^f \frac{\partial C}{\partial x_i} - \frac{\partial}{\partial x_i} \left(D_{ij} \frac{\partial C}{\partial x_j} \right) + (R\vartheta + Q_\rho) C = Q_C. \quad (5)$$

With the constitutive equations

$$\rho^f = \rho_0^f \left[1 + \frac{\bar{\alpha}}{(C_s - C_0)} (C - C_0) - \bar{\beta} (T - T_0) \right], \quad (6)$$

$$h = \frac{p^f}{\rho_0^f g} + x_t, \quad (7)$$

$$K_{ij} = \frac{k_{ij} \rho_0^f g}{\mu_0^f}, \quad (8)$$

$$\bar{\alpha} = \frac{[\rho^f(C_s) - \rho_0^f]}{\rho_0^f}, \quad (9)$$

$$f_\mu = \frac{\mu_0^f}{\mu^f(C, T)}, \quad (10)$$

$$D_{ij} = \left(\varepsilon D_d + \beta_T V_q^f \right) \delta_{ij} + (\beta_L - \beta_T) \frac{q_i^f q_j^f}{V_q^f}, \quad (11)$$

$$R = \varepsilon + (1 - \varepsilon) \chi(C), \quad (12)$$

$$R_d = \varepsilon + (1 - \varepsilon) \frac{\partial [\chi(C) \cdot C]}{\partial C}, \quad (13)$$

where h is the hydraulic head, q_i^f is the Darcy velocity vector of fluid, C is the concentration of the chemical component, T is the temperature, ρ^f is the density of the fluid, ρ_0^f is the density of the reference fluid, K_{ij} is the tensor of hydraulic conductivity, f_μ is the constitutive viscosity relation function, R is the retardation factor, R_d is the derivative term of retardation, D_{ij} is the tensor of hydrodynamic dispersion, ε is the porosity, c_f , c_s is the specific heat capacity of fluid and solid, respectively, α is the fluid density difference ratio, β is the fluid expansion coefficient, C_0 , T_0 are the reference concentration and temperature, respectively, C_s is the maximum concentration, p^f is the fluid pressure, g is the gravitational acceleration, k_{ij} is the tensor of permeability, μ^ϕ , μ_0^f are the dynamic viscosity and its reference value, respectively, of fluids, D_d is the molecular diffusion coefficient of fluid, V_q^f is absolute Darcy fluid flux, β_L , β_T are longitudinal and transverse dispersivity, and $\chi(C)$ is the concentration-dependent adsorption function.

Parameters that are necessary to consider the density difference in groundwater were assigned to the 3D-groundwater model, to account for the freshwater–seawater interactions. The hydraulic head at the Bay of Bengal boundary was considered as a saltwater head, to account for the difference in pressure between freshwater and seawater. This boundary was assigned with a concentration of 19,500 mg/l since this was the concentration of chloride in seawater. The total dissolved solids in groundwater of the western boundary of 800–1200 mg/l (Indu et al. 2013) were assigned as the variable head boundary. An initial concentration of chloride distributed in both the aquifers was assigned based on the measurements made by the Tamil Nadu Public Works Department in wells with the screens in different depths. To evaluate the density gradient near the coast at a finer resolution, the eastern part of the area was discretized into much smaller cells of size varying from 200 to 800 m². The density of freshwater and seawater were considered as 1000 kg/m³ and 1025 kg/m³, respectively. Longitudinal dispersivity, transverse dispersivity, and coefficient of molecular diffusion were initially considered as 66.6 m, 6.6 m, and 1×10^{-6} m²/s, respectively, as reported by Sherif and Singh (1999) in the same study area.

Management options to mitigate the seawater intrusion

The model was used to identify suitable measures to understand and restore the groundwater head by increasing the rainfall recharge and reduction of pumping. However, further reduction in groundwater pumping in this region is difficult, as the livelihood of farmers will be affected apart from the reduction in well field pumping. Hence, an increase in groundwater recharge is a viable alternative to cope up with the problem of seawater intrusion. The groundwater recharge can be improved to prevent seawater intrusion by several methods such as spreading ponds, modification of pumping pattern, artificial recharge, extraction barrier, injection barrier, and subsurface barrier (Todd and Mays 2005). The groundwater depletion in this area can be overcome by increasing the recharge and already managed aquifer recharge schemes have been initiated by the construction of check dams across the two rivers. So the model runs under different scenarios of increasing the recharge to identify measures to mitigate seawater intrusion. The scenarios considered are

- Scenario 1: with additional check dams (based on the topography and river morphology six check dams are suggested).
- Scenario 2: with additional check dams and 1 m increase in crest level of all check dams.

- Scenario 3: rejuvenation of defunct water bodies with scenario 2.
- Scenario 4: termination of pumping in five well fields with scenario 3.

Results

Simulation of rainfall–runoff model (NAM)

A–K basin characteristics

The river basin is defined as the topographical area which receives rainfall and drains the runoff water through a single outlet. The sub-catchments of the A–K basin were first delineated, to estimate the runoff and discharge rate. For this purpose, a morphological analysis was carried out in the A–K river basin by using the hydrological tool, namely ArcHydro in ArcGIS 10.2. The digital elevation model (DEM) generated from the SRTM data (Fig. 8a) was used to create flow direction, accumulation of water in depressions, creation of stream networks, and delineation of watersheds. First, the downloaded DEM was processed to fill all the cells with respect to the neighboring cells (Fig. 8b). The flow direction map was created by matching the elevation difference between the neighboring cells (Fig. 8c). Next, a flow accumulation map was created by finding the flow path of every cell on the basin (Fig. 8d). The river channels and surface water divides were identified from the flow accumulation values. The cells with high values represent the river channel and the cell with zero accumulation shows ridges. The next step is to assign a unique number to each link in the stream raster and then give a stream order based on the Strahler method of stream order. The stream order map arrived by this method is shown in Fig. 8e. Finally, the sub-catchments were created from stream order and pour point. Figure 8f shows the sub-catchments of the A–K basin which is considered for the rainfall–runoff (NAM) model.

Two separate rainfall–runoff models were built for each Araniyar and Korttalaiyar catchments and NAM model parameters were calibrated based on the availability of discharge data in the catchment. Daily discharge data for 9 years (2004–12) were obtained from the Chennai Metropolitan Water Supply and Sewerage Board website and used for calibrating the model. In addition, the discharge data model was also calibrated on the range of minimum and maximum annual recharge estimated values obtained from previous studies (Anuthaman 2009; Sivaraman and Thillai-govindaranjan 2012) in the catchment as a percentage of total annual rainfall. During calibration, the optimal model parameters are estimated by manually fine-tuning within the allowable range with the option of automatic calibration (Kumar et al. 2019). The surface root zone and groundwater

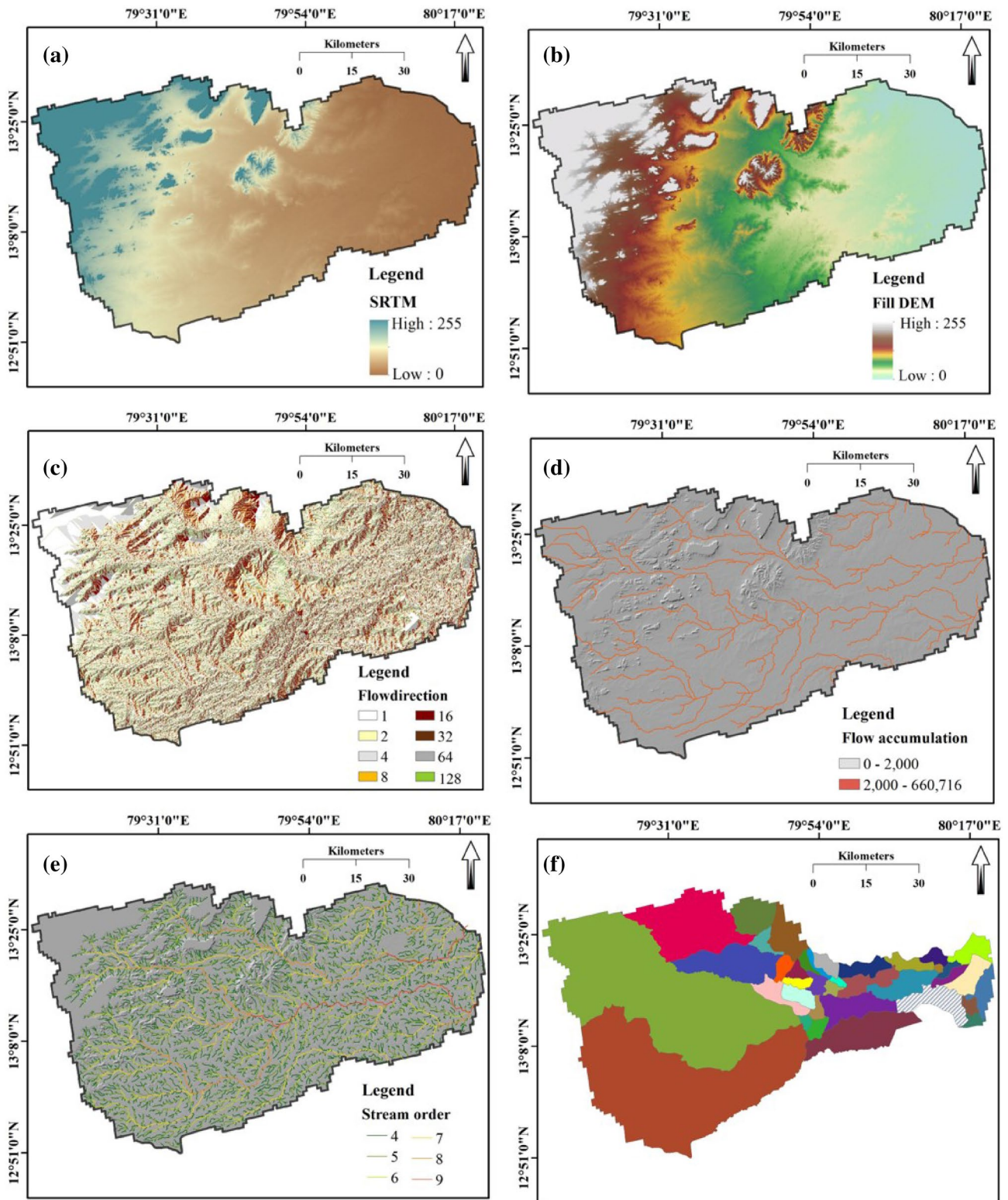


Fig. 8 Delineation of A–K sub-basin from SRTM downloaded from USGS **a** digital elevation model, **b** filled DEM, **c** flow direction of the study area, **d** flow accumulation, **e** stream order and **f** sub-catchments of the study area used for rainfall–runoff model

Table 2 Surface and root zone parameters after calibration (Bhola 2012)

Name	Area (km ²)	U_{max} (mm)	L_{max} (mm)	CQOF	CKIF (h)	CK _{1,2} (h)	TOF	TIF
Arani catchment	1490.90	35	600	0.15	800	15	0.05	0.2
Kortallaiyar catchment	1300.10	35	600	0.15	800	15	0.05	0.2

Table 3 Groundwater parameters after calibration (Bhola 2012)

Name	Area (km ²)	TG	CKBF (h)	C_{area}	S_y
Arani catchment	1490.90	0.1	300	0.4	0.1
Kortallaiyar catchment	1300.10	0.1	300	0.4	0.1

parameters after the calibration are shown in Tables 2 and 3. The model calibration was carried out for 9 years (limited to data availability) to verify the ability of the model to predict different streamflow conditions. The accuracy of MIKE11 NAM was evaluated based on the coefficient of determination (R^2) (Hafezparast et al. 2013), and the obtained R^2 value is 0.65 (Fig. 9). The simulated and observed streamflow is compared in Fig. 9. The model predicts the river flow with a reasonable level of accuracy during the periods of normal flow. The model predicts in excess of total volume by 10.5% in 8 years and a peak error of nearly 7% for a discharge greater than 300 m³/day.

Simulation of surface water model (MIKE 11 HD)

The MIKE 11 HD model was set up to simulate the water level in the two rivers based on the rainfall. Further, the impact of the check dams on the water level in the river was also simulated. The model was tested successfully on numerical stabilities and described all the basic functionality, e.g., the effect of integrated structures, diversions, and reservoirs in a realistic way. The capability of the model was improved by including 30 m resolution digital elevation data,

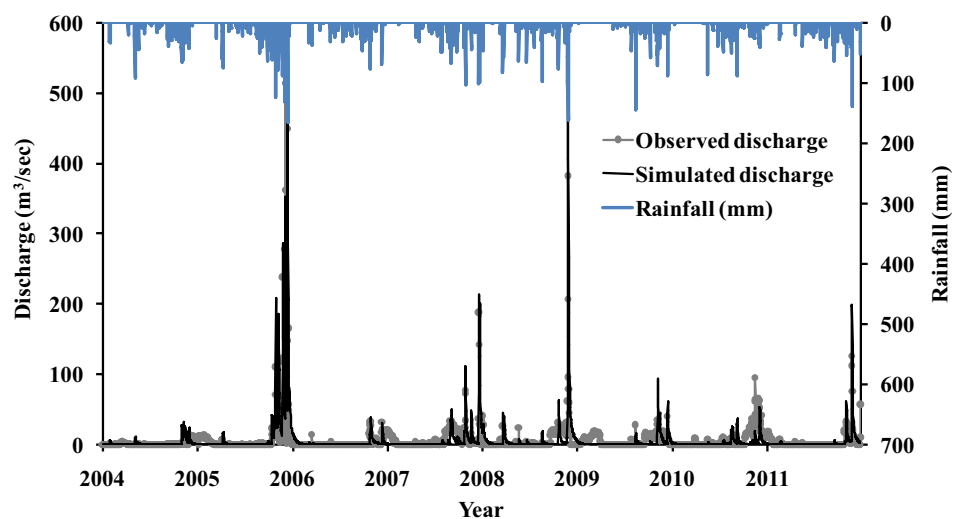
improvement of the bathymetry of the rivers, and installing more gauging stations in the A–K basin (especially, upstream rainfall stations and discharge stations at important check dams and junctions). The model was used to simulate the discharge and water level at specified points along the rivers. The effect of reservoirs and canals was also considered while modeling. The results obtained by the MIKE 11 HD are thus dependent on the results of NAM catchments (Fig. 10). The downward arrows represent that sub-catchments are coupled to the river at these locations (Fig. 10).

Simulation of groundwater flow

Model calibration

The model was calibrated in two stages: steady and transient-state condition. The steady-state calibration was carried out by varying the aquifer parameters within the allowable range (plus or minus 10%) to obtain a good match between the observed and simulated groundwater head. The range of values of aquifer parameters considered for modeling is given in Table 4. The spatial distribution of hydraulic conductivity values in the unconfined, aquitard, and semi-confined aquifer regions are shown in Fig. 11. A number of trial runs were made to minimize the difference between the observed and the simulated groundwater head. The groundwater model was successfully calibrated under steady state and the R^2 values for the regression line drawn between observed and simulated head for unconfined and semi-confined aquifer were 0.990 and 0.901 respectively (Fig. 12). Transient calibration

Fig. 9 Temporal variation in rainfall, observed and simulated discharge in a sub-catchment. (Data source: Bhola (2012))



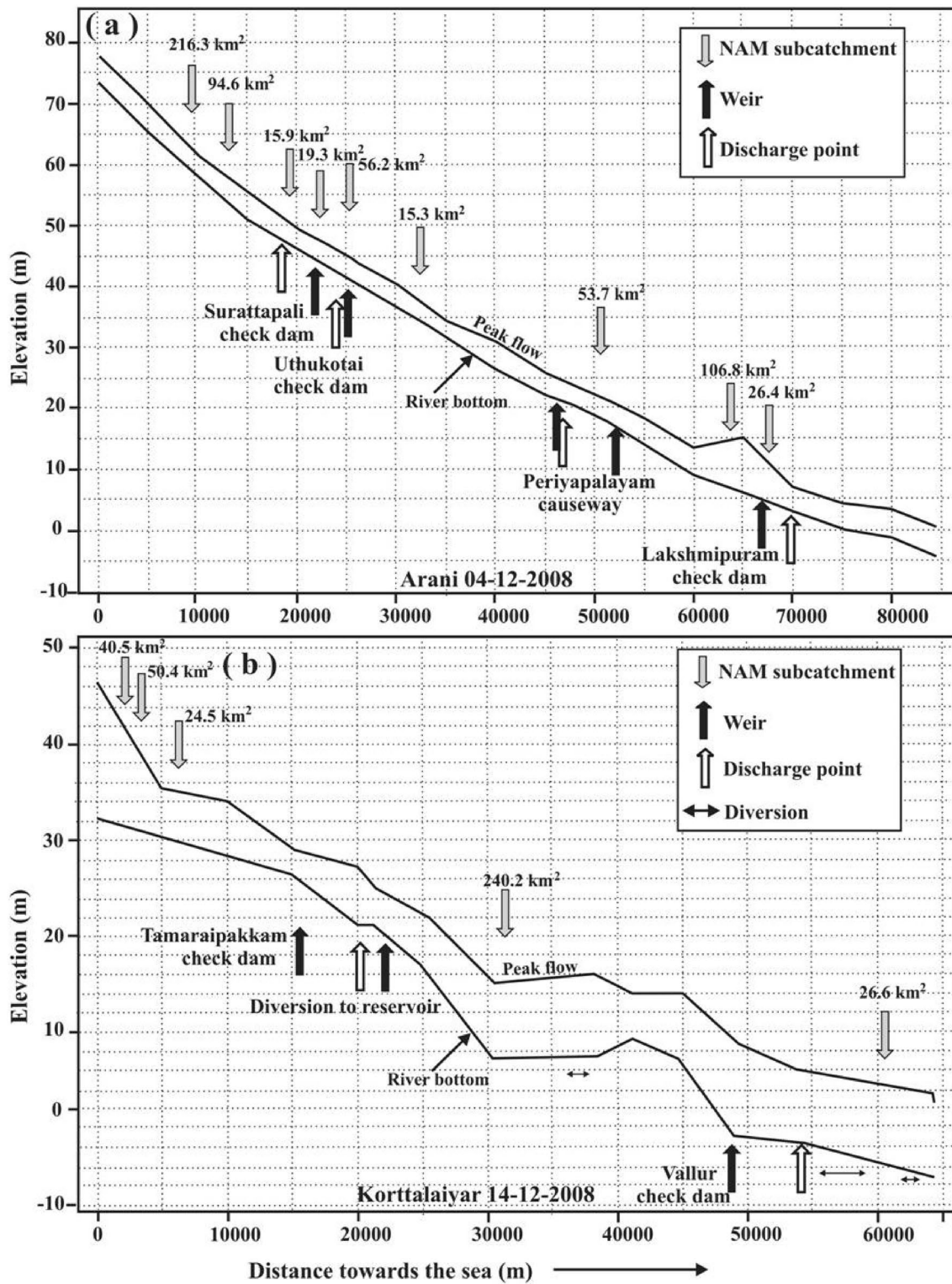


Fig. 10 Rainfall–runoff model linked to surface water model, i.e., a Arani and b Korttalaiyar rivers. (Data source: Bhola (2012))

was carried out for a period from January 1996 to December 2003. Transient-state calibration was conducted by a trial and error method until the best possible comparison was

obtained between the observed and the simulated groundwater head by slightly varying the aquifer parameters. After the transient-state calibration, the R^2 values for the regression

Table 4 Initial and calibrated hydraulic conductivity and storage coefficient values

Geology/pumping test locations	Hydraulic conductivity, K (m/day)		Specific yield/storage coefficient	
	Initial	Calibrated	Initial	Calibrated
Unconfined aquifer (based on the geology)				
Silty sand	40–100	35–100	0.10	0.12
Clayey sand	50	65	0.06	0.08
Laterite	5	4	0.025	0.03
Sandstone and conglomerate, with calcareous gritstone	75	72	0.09	0.06
Semi-confined aquifer (based on pumping tests (UNDP 1987))				
Kattur	75	100	8×10^{-3}	8.5×10^{-3}
Interface	118	100	2.5×10^{-3}	3×10^{-3}
Northeast Minjur	228	250	5.0×10^{-3}	6.0×10^{-3}
Duranallur	69	50	1.4×10^{-3}	2×10^{-3}
West of Panjetti	118	85	7×10^{-3}	8×10^{-3}

line was 0.993 and 0.901 between the observed and the simulated heads in the unconfined and semi-confined aquifers, respectively (Fig. 13).

Model validation

The calibrated model was later validated with the input parameters derived from calibration from the year January

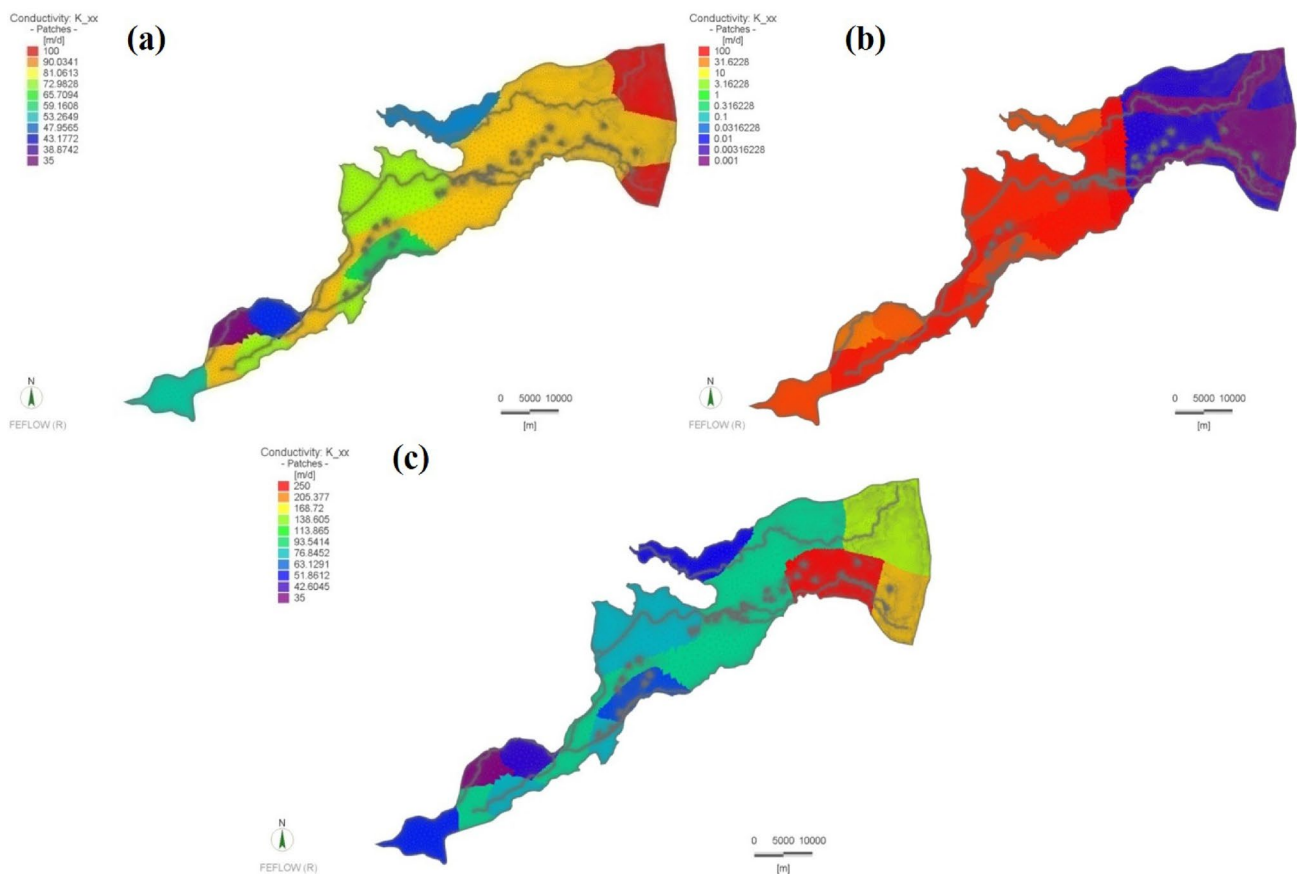
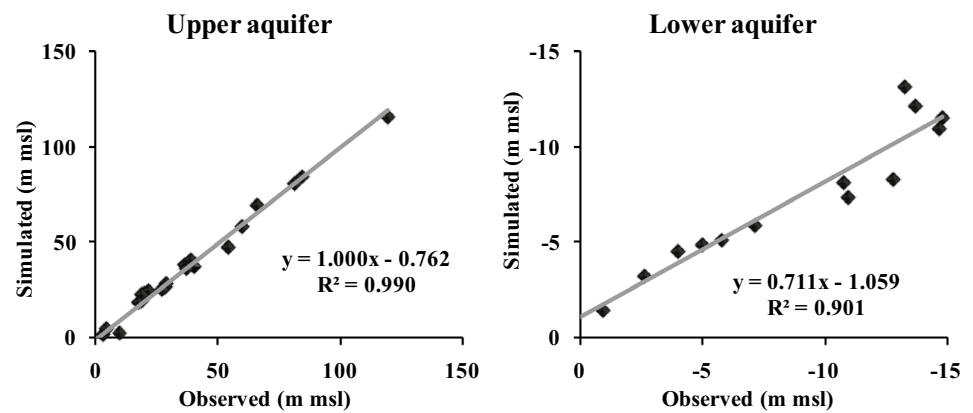


Fig. 11 Spatial distribution of hydraulic conductivity values in m/day **a** in the unconfined aquifer, **b** in the unconfined aquifer (west) and aquitard (east), **c** in the unconfined aquifer (west) and semi-confined aquifer (east)

Fig. 12 Comparison of observed and simulated groundwater heads under steady-state calibration



2004 to December 2012. A realistic match was obtained between the observed and the simulated groundwater head. This indicates that the model with the assigned input parameters is able to reproduce the observed heads and thus the prediction capacity of the model was tested. The time series of the observed and the simulated groundwater heads for the wells in the unconfined aquifer during calibration and validation periods are shown in Fig. 14a. Observed and simulated groundwater heads in the semi-confined aquifer well field wells during calibration and validation are shown in Fig. 14b. The figure indicates that the groundwater head started decreasing in the semi-confined aquifer from the year 2002 and severe decline occurred in the years 2004 and 2005.

The advantage of this integration can be understood by comparing the simulated values with observed values (Fig. 15). The groundwater head simulated by the simple groundwater model is much lower than the groundwater head derived from the integrated model. Further, the effect of peak runoff in the groundwater head is very well brought out in the integrated model, as the amount of rainfall–runoff and infiltration from the rivers were considered directly from surface water model, which gives more accurate results compared to the non-integrated model. An integrated approach only will be able to predict the groundwater flow

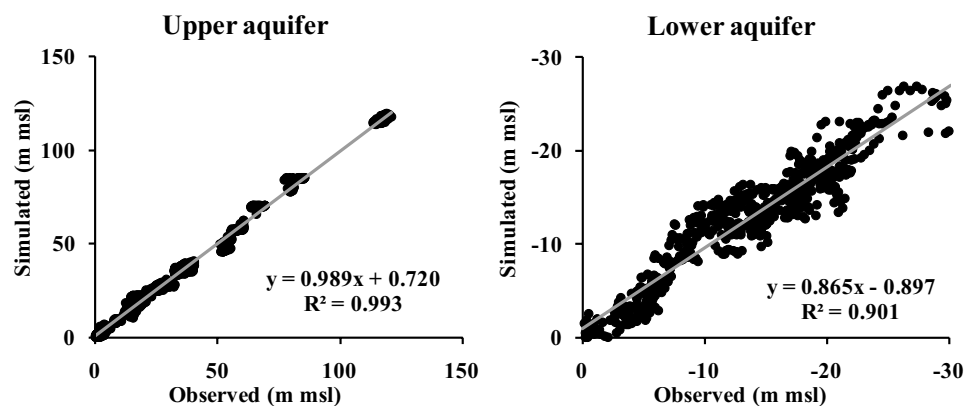
by considering the timing of rainfall, resulting in runoff and infiltration. Such a study is very important for coastal aquifers, as the groundwater from these aquifers is used for various purposes and overextraction results in seawater intrusion.

Simulation of density-dependent seawater intrusion

Model calibration

The chloride concentration was calibrated under steady- and transient-state conditions. The steady-state calibrated result of simulated chloride values was compared with the measured value of chloride (Fig. 16). It shows a reasonable match between the measured and simulated chloride concentration with the regression value of 0.808. Since no measured chloride concentration was available for the semi-confined aquifer, such a comparison could not be made. Then, transient-state calibration was carried out from January 1996 to December 2004. A number of runs were carried out by considerably varying the longitudinal and transverse dispersivity values by a trial and error method, for comparing the measured and simulated chloride values. After several simulations, finally, a reasonable match between the

Fig. 13 Comparison of observed and simulated groundwater heads under transient-state calibration



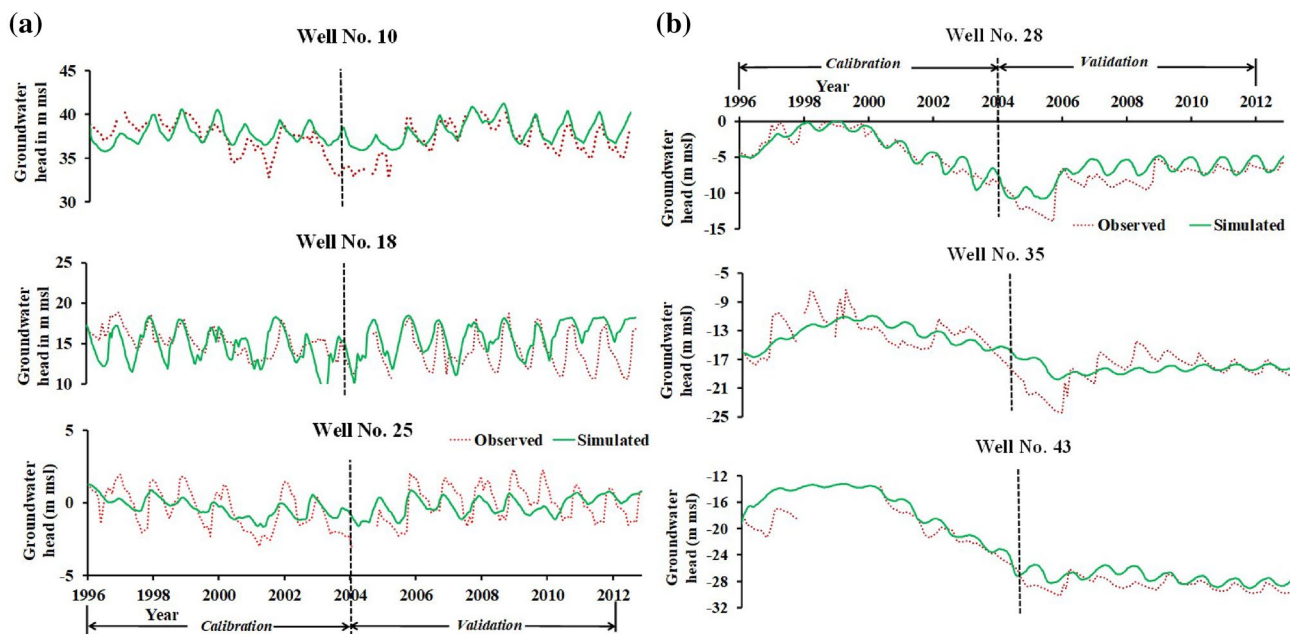
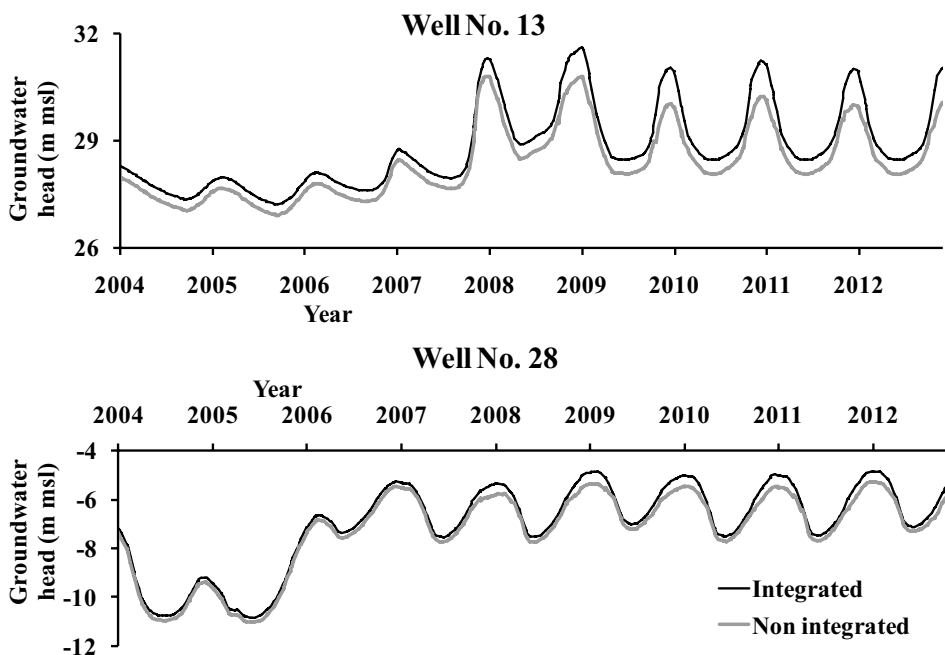


Fig. 14 Temporal variation in observed and simulated groundwater head (m msl): a unconfined aquifer and b semi-confined aquifer

Fig. 15 Comparison of simulated groundwater head for integrated and non-integrated modeling in unconfined (well no. 13) and semi-confined (well no. 28) aquifer



measured and the simulated values was obtained with the longitudinal and transverse dispersivity values of 70 m and 7 m, respectively. Temporal variations in the measured and simulated concentration of chloride from some of the wells located in the unconfined aquifer are shown in Fig. 17. The accuracy of the measured and simulated chloride concentrations was examined quantitatively on the basis of coefficient of determination (R^2). The coefficient of determination value

shows 0.80 (Fig. 16), which describes best match between the measured and simulated values.

Model simulation

Simulation of the density-dependent seawater intrusion was carried out by using an automatic time step method with an initial time step length of 0.001 days from January 2000 to

Fig. 16 Comparison of the measured and simulated chloride concentration: **a** steady-state and **b** transient-state calibration

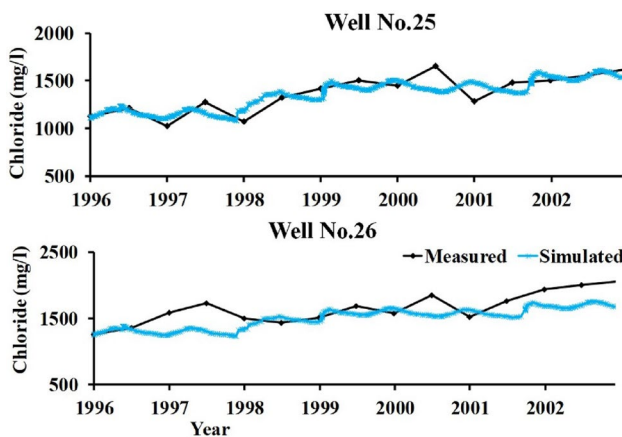
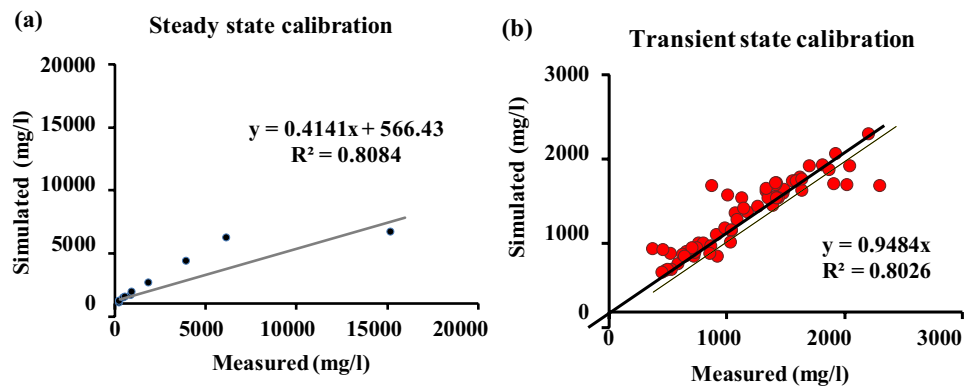


Fig. 17 Temporal variation in the measured and simulated chloride concentration in the unconfined aquifer

December 2012. The simulated west to east cross section for a distance of about 30 km from the coast, along with the monitoring of well no. 28 to coast for the months of January and June for the years 2000, 2005 and 2010 are shown in Figs. 18 and 19. This figure shows the discontinuous line around -15 m which represents the separation of chloride concentrations in the two aquifer system. The semi-confined aquifer has fresh groundwater from top to a depth of about 5 m, indicating less chloride values in the dark blue color.

Sensitivity analysis

Sensitivity analysis is the method of changing the model input parameters within a reasonable range to evaluate the responses on model prediction. Sensitivity analysis is used to recognize the influence of input parameters on the simulated groundwater head and also to understand the sensitivity of one input parameter compared to other input parameters. Sensitivity analysis was carried out for the input parameters such as horizontal hydraulic conductivity, vertical hydraulic conductivity, and specific storage by an increase

and decrease of 10%. Groundwater head increases by about 0.4–2.0 m and decreases by about 0.2–1.0 m while decreasing and increasing the horizontal hydraulic conductivity by 10%, respectively, in the unconfined aquifer. Groundwater head increases by about 1.5–3.0 m and decreases by about 1.5–5.0 m while increasing and decreasing the horizontal hydraulic conductivity by 10%, respectively, in the semi-confined aquifer. Groundwater head increases and decreases by about 0.1–0.4 m while increasing and decreasing the vertical hydraulic conductivity by 10% in the unconfined aquifer. As the increase in vertical hydraulic conductivity will result in increase in vertical flow from the unconfined aquifer to the semi-confined aquifer and the groundwater head decrease in the unconfined aquifer, it increases the head in the semi-confined aquifer. Hence, the increase in the vertical hydraulic conductivity by 10% results in rise in the groundwater head by 0.6 m in the semi-confined aquifer. There is no significant difference in the simulated groundwater head while changing the specific storage by $\pm 10\%$. Table 5 explains the response of aquifer for change in aquifer parameters. The result shows that there is a maximum groundwater head of about 1.5–3 m increase in the semi-confined aquifer for 10% increase in horizontal hydraulic conductivity, and the maximum groundwater head of about 0.2–2 m increase in the unconfined aquifer for 10% decrease in horizontal hydraulic conductivity. From sensitivity analyses, it is understood that the horizontal hydraulic conductivity is a very sensitive parameter; however, it was estimated with a reasonable level of accuracy by the UNDP (1987).

Mitigation measures for seawater intrusion

Rajaveni et al. (2016) simulated the non-integrated model to find the response of groundwater recharge and pumping in seawater intrusion in the same study area. Figure 20 shows that the predicted groundwater head by the model under scenarios 1, 2, 3, and 4 in a well located in the unconfined and semi-confined aquifer. The model predicts that in the unconfined aquifer, the groundwater head will be

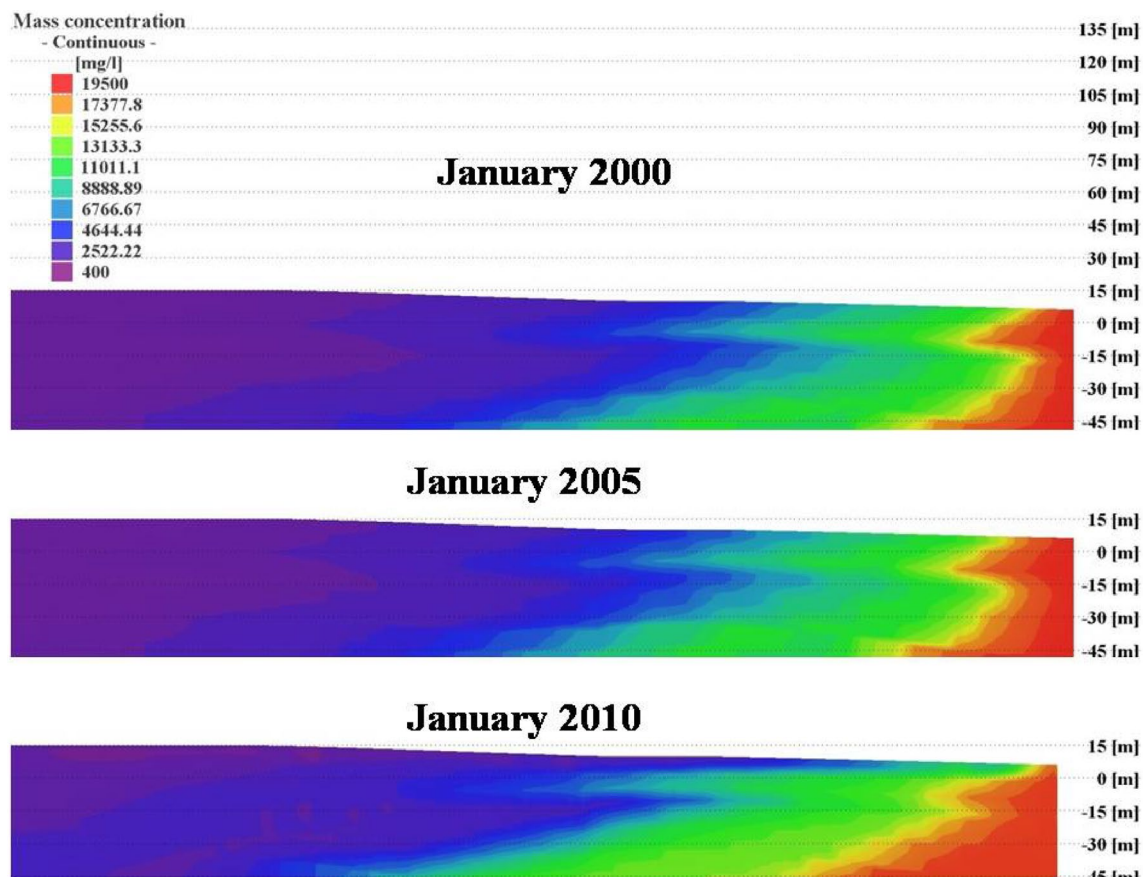


Fig. 18 Simulated variation in chloride concentration from west to east cross section during January 2000, 2005, ad 2010

increased by about 2 m by the construction of six additional check dams as in scenario 1. The groundwater head will be increased by about 2.8 m while considering an increase of the crest level of the dams by 1 m (scenario 2). The groundwater head will be increased by about 3.8 m if all the non-operational water bodies are rejuvenated as in scenario 3. Prediction with scenario 3 indicates that the implementation of recharge structures alone is not sufficient to restore this aquifer system affected by seawater intrusion. Hence, the reduction in pumping from well fields, which supply water to Chennai City, was considered to predict the groundwater head during 2030.

Simulation under scenario 4 indicates an increase in groundwater head by about 4.2 m if the groundwater pumping from five well fields was stopped in the year 2016. Thus the implementation of additional check dams, increase in the crest level of check dams by 1 m, rejuvenation of the water bodies and termination of pumping in five well fields will result in an increase in groundwater head by about 4.2 m by the end of the year 2030 in the unconfined aquifer. In the semi-confined aquifer, the groundwater head will increase by 1.5 m for scenario 1, 1.8 m for scenario 2, 2.3 m for scenario 3, and 7.5 m for scenario 4. Even though the identified

locations for the additional check dams are in regions with the two-aquifer system, the leakage from the unconfined aquifer to the semi-confined aquifer results in an increase in groundwater head of the semi-confined aquifer.

Figure 21 shows the predicted chloride concentration by the model under scenarios 1, 2, 3, and 4 in a well located in the unconfined and semi-confined aquifer. Scenarios 1, 2, and 3 show a lesser amount of about 100–250 mg/l chloride concentration was diluted compared to scenario 4. The predicted results show that the concentration of chloride values decreased with a minimum of about 500 mg/l and a maximum of about 1100 mg/l in the unconfined aquifer in scenario 4. In the semi-confined aquifer, the chloride concentration decreased with a minimum of about 250 mg/l and a maximum of about 800 mg/l in scenario 4.

Discussion

In the present study, an integrated modeling approach was constructed for the coupling surface and groundwater processes. This consists of the rainfall–runoff model (NAM) producing surface flow for river model (MIKE 11 HD). It

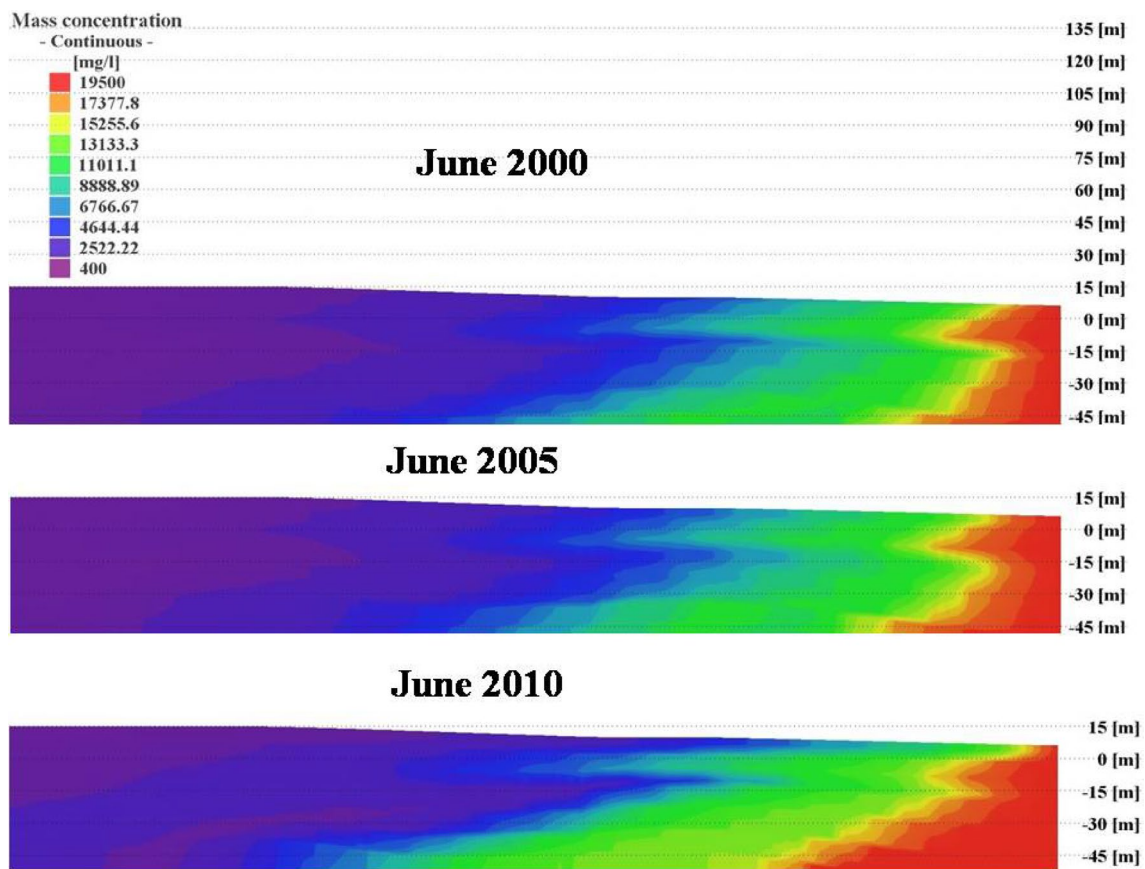


Fig. 19 Simulated variation in chloride concentration from west to east cross section during June 2000, 2005, and 2010

Table 5 Sensitivity analysis of parameters and root mean square error (+ symbol indicates increasing percentage and groundwater head. - symbol indicates decreasing percentage and groundwater head)

Parameter	Change in %	Change in groundwater head (m)		RMSE	
		Unconfined aquifer wells	Semi-confined aquifer wells	Unconfined aquifer wells	Semi-confined aquifer wells
Horizontal hydraulic conductivity	+ 10	-0.2 to -1.0	+1.5 to +3.0	-1.20	3.20
	- 10	+0.2 to +2.0	-1.5 to -5.0	2.30	-5.25
Vertical hydraulic conductivity	+ 10	+0.1 to +0.4	+0.1 to +0.4	1.00	1.00
	- 10	-0.1 to -0.4	-0.1 to -0.4	-0.88	-0.88
Specific storage	+ 10	+0.05 to +0.15	+0.05 to +0.15	0.10	0.10
	- 10	-0.05 to -0.15	-0.05 to -0.15	-0.10	-0.10

includes the already existing check dam structures. The river flow model (MIKE 11 HD) is connected to the groundwater model (FEFLOW) through the coupling interface (ifm-MIKE11). Density-dependent flow processes were included in the groundwater model after the successful calibration of the single and integrated models.

The rainfall–runoff modeling result shows that the model overestimates the quantity of flow during heavy rainfall. This discrepancy was solved by simulating rainfall–runoff for long

periods of time. The accuracy of the rainfall–runoff model can be improved by considering the snowfall coefficient for simulation (Lafdani et al. 2013). The current research was carried out in the tropical region, which does not include the snowfall coefficient. The rainfall–runoff model was used to generate the runoff of all the catchments and infiltration with hourly time steps, which was later corrected monthly to link it with the regional river flow model. The results of the river flow model show that the effect of the reservoir outcome in a

Fig. 20 Predicted groundwater head in the unconfined and semi-confined aquifer under four scenarios considered

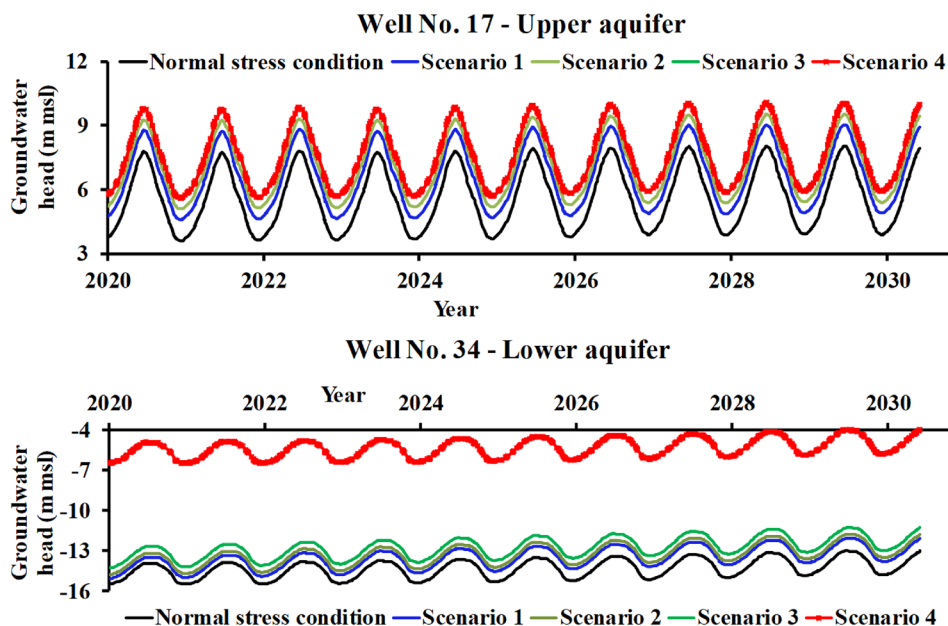
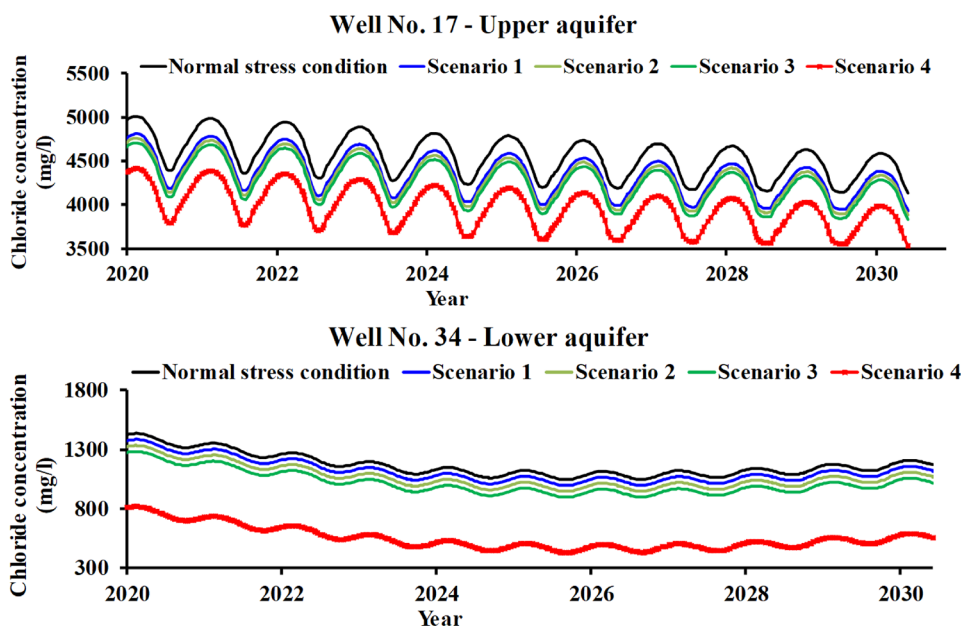


Fig. 21 Predicted chloride values in the unconfined and semi-confined under four scenarios considered



drop of peak discharge as water is diverted to the Cholavaram reservoir. The Poondi reservoir controls the excess discharge in the Korttalaiyar River. The increment in bigger catchments is much more when compared to the smaller catchments. Also, Cappelaere et al. (2003) pointed out that the computed annual discharge mainly depends on the number of events and rain intensities than on annual rainfall.

The above-mentioned coupled model was again linked to the groundwater model. The simulated groundwater head in Fig. 14a, b indicates the severe decline in the semi-confined aquifer during the years 2004 and 2005. The CMWSSB, which pumps the groundwater from well fields during low rainfall

years (2002–2004), has stopped pumping from Minjur and Panjetty well fields due to this huge decline in the head. Due to the termination of pumping from these well fields in the year 2005, the groundwater head started to increase in the year 2006. However, the groundwater head is still at – 30 m sl (Well No. 43). Since the groundwater head is below the sea level, this region has been affected by seawater intrusion.

During the year 2000, the seawater (groundwater with chloride of 1000 mg/l) has intruded up to a distance of 10 km in the unconfined and 12 km in the semi-confined aquifer (Rajaveni et al. 2016). The monsoon rainfall could only push 200 m, which could be observed in January 2005.

The seawater intrusion was very high in the year 2005 due to the overextraction of the groundwater in the summer months of April and May when the head has decreased to about -30 m (Fig. 14). Due to this reason, the groundwater pumping from the Minjur and Panjetty well fields was terminated in the year 2005 as explained earlier. This has resulted in only a marginal improvement in chloride concentration in the year 2010. The simulated variation in chloride by the density-dependent modeling indicates that a distance of about 15 km has been affected by seawater intrusion. Hence, it is necessary to properly manage this aquifer system to mitigate the problem of seawater intrusion. The developed model was used to identify possible management measures to mitigate seawater intrusion.

The interaction with the river model increases the simulated groundwater heads bypassing the effect of the peak flows in combination with the check dams and interlinking of rivers into the groundwater model. This process would have been underestimated by the non-integrated groundwater model, showing the advantage of using such an integrated model (Fig. 15). The integrated model increased the groundwater head of about 1 m during the post-monsoon months (December and January), because of the impact of real-time coupling of hydrological processes after rainfall. Zhang and Li (2009) compared lumped conceptual models with an integrated surface runoff and groundwater flow model. This integrated simulation showed more detailed information on components of groundwater recharge and base flow, as well as the dynamics of groundwater flow.

After the comparison of the integrated and non-integrated model, the developed model was used to analyze several scenarios, including the construction of additional check dams, increasing the crest level of the check dams, rejuvenation of non-operational water bodies, and reducing the abstraction by limiting the pumping in some of the well fields. The predicted result shows a groundwater head increase of about 7.5 m (Fig. 20) at a distance of 20 km from the coast, while the groundwater head rises by 12 m at a distance of 5 km (Well No. 34) from the coast in the semi-confined aquifer under scenario 4. The maximum reduction of chloride concentration was about 1100 mg/l and 800 mg/l in the unconfined and semi-confined aquifers, respectively. The dissolution of chloride concentration is more in the unconfined aquifer compared to the semi-confined aquifer, because managed aquifer recharge structures are very much subjective to unconfined aquifer conditions of the unconfined aquifer. The stopping of well field pumping only provides more dissolution of chloride concentration in the semi-confined aquifer.

Rajaveni et al. (2016) identified that the 10% increase in rainfall recharge and 10% decrease in pumping show greater impact on the groundwater head of about 3 m rise in the unconfined aquifer and 6 m rise in the semi-confined aquifers, respectively. Hence, this realtime integration between

rainfall, runoff, surface water and groundwater provides accurate amount of available water in this aquifer, which helps in the management of water resources. Torres-Martine et al. (2019) identified that the absence of long drought periods, implementation of recharge wells, and hurricanes should be taken together for the mitigation of seawater intrusion further or to drive back of the freshwater–seawater interface to the coastline.

The simulation results indicate that the most effective aquifer recharge is reached by including additional check dams, but even with combined increased dam crest levels and rejuvenation of non-operational water bodies, this is not sufficient to restore the aquifer with respect to seawater intrusion. A positive local effect of the MAR structures and reduction in pumping were identified both on the groundwater levels and in pushing back the saltwater front. It shows that a reduction of the current abstraction rate is necessary for sustainable management of the existing water resources. This tool can be used for the long-term analysis of MAR structures by using current seasonal cycles of climatological and groundwater recharge conditions. It can also be used for predicting seasonal variations through climate change conditions as well as for general water resource quantifications.

Conclusion

Integrated rainfall–runoff, infiltration, surface water, and density-dependent models are useful in the identification of measures to mitigate seawater intrusion in a coastal aquifer. Data requirements to parameterize such models are more important for the realistic simulation of density-dependent seawater intrusion to study to effect of managed aquifer recharge structures. The important outcomes of this work are as follows.

1. Rainfall–runoff model (NAM) was constructed using 8 years of daily discharge data from Poondi reservoir. Since the model has been optimized over an 8-year time period, it covers a wide range of hydrologic and climate conditions, creating confidence in the ability of the model to forecast streamflow conditions in a number of scenarios. A satisfactory comparison with observed flow values with R^2 value of 0.6 was achieved by the model.
2. The surface water model (MIKE 11 HD) has been successfully tested with numerical stabilities and describes all the basic functionality, e.g., the effect of integrated structures, diversions and reservoirs in a realistic way. In the Korttalaiyar River, the effect of the reservoir results in a drop of peak discharge as water is diverted to the Cholavaram reservoir. The Poondi reservoir controls the excess discharge in Korttalaiyar.

3. The successfully calibrated integrated density-dependent groundwater model (FEFLOW) was used to investigate the best management options to mitigate the seawater intrusion by different scenarios, because the seawater had intruded by about 15 km in the semi-confined aquifer due to heavy pumping from well fields constructed by Chennai Metropolitan Department and higher hydraulic conductivity compared with the unconfined aquifer.
4. The management option of increasing the crest level of existing check dam by 1 m, construction of six additional check dams, rejuvenation and cleaning of the existing water bodies, and termination of pumping from well fields increases the groundwater head by about 7.5 m, the chloride concentration to about 800 mg/l in the semi-confined aquifer by the end of the year 2030. Thus, in spite of considering all the possible measures, the model predicts that the seawater–freshwater interface helps to dissolve salinity concentration and desalinizes groundwater for about 5 km, which makes groundwater potable.

Acknowledgements The co-funding for the collaborative project ‘Enhancement of natural water systems and treatment methods for safe and sustainable water supply in India—SaphPani’ (www.saphpani.eu) from the European Commission within the Seventh Framework Programme (Grant agreement number 282911) is gratefully acknowledged. The Department of Science and Technology, New Delhi, India (Grant no: DST/WAR-W/SWI/05/2010) is kindly acknowledged. The authors wish to acknowledge the Tamil Nadu Public Works Department, Chennai Metropolitan Water Supply and Sewerage Board, India, for providing the necessary groundwater level and bore hole data.

References

- Amir MSII, Khan MMK, Rasul MG, Sharma RH, Akram F (2013) Numerical modelling for the extreme flood event in the Fitzroy basin, Queensland, Australia. *Int J Environ Sci Dev* 4(3)
- Anuthaman NG (2009) Groundwater augmentation by flood mitigation in Chennai region—a modelling based study. Ph.D Thesis, Anna University, Chennai, India
- Bhadra A, Bandyopadhyay A, Singh R, Raghuvanshi NS (2010) Rainfall–runoff modeling: comparison of two approaches with different data requirements. *Water Resour Manag* 24:37–62
- Bhola PK (2012) Hydrological and hydraulic modelling of ungauged Araniyar—Kortalaiyar River Basin, Chennai, India. Master thesis
- Bizhanimanzar M, Leconte R, Nuth M (2020) Catchment-scale integrated surface water-groundwater hydrologic modelling using conceptual and physically based models: a model comparison. *Water* 12:363. <https://doi.org/10.3390/w12020363>
- Cappelaere B et al (2003) Associating uncertain data and uncertain models—an experiment in a small Sahelian basin. In: Servat E, Najem W, Leduc C, Shakeel A (eds) *Hydrology of Mediterranean and semiarid regions*, vol 278. IAHS Press, Wallingford, pp 151–156
- Charalambous AN, Garratt P (2009) Recharge–abstraction relationships and sustainable yield in the Arani-Kortalaiyar groundwater basin, India. *Q J Eng Geol Hydrogeol* 42:39–50
- DHI (2005) MIKE 11 – A modelling system for Rivers and Channels. Short introduction tutorial, Denmark. Danish Hydraulic Institute
- DHI (2007) MIKE 11 User manual. DHI Water and Environment, Demark, pp 229–2441
- DHI (2009) Finite element subsurface flow and transport simulation, white paper, vol 1. DHI
- DHI (2017) MIKE 11: a modeling system for rivers and channels. DHI
- Ferguson G, Gleeson T (2012) Vulnerability of coastal aquifers to groundwater use and climate change. *Nat Clim Change Adv* 2:342–345. <https://doi.org/10.1038/NCLIMATE1413>
- Furman A (2008) Modeling coupled surface–subsurface flow processes: a review. *Vadose Zone J*. <https://doi.org/10.2136/vzj2007.0065>
- GEC (1997) Groundwater resources estimation methodology 1997: report of the groundwater resources estimation committee. Ministry of water resources, New Delhi, p 100
- Guzha CA, Hardy TB (2010) Simulating streamflow and water table depth with a coupled hydrological model. *Water Sci Eng* 3:241–256
- Hafezparast M, Araghinejad S, Fatemi SE, Bressers H (2013) A conceptual rainfall–runoff model using the auto calibrated NAM models in the Sarisoo River. *Hydrol Curr Res* 4:1. <https://doi.org/10.4172/2157-7587.1000148>
- Harbaugh AW, Banta ER, Hill MC, McDonald MG (2000) MODFLOW-2000. The US geological survey modular ground-water model—user guide to modularization concepts and the ground-water flow process. Geological Survey, Preston County
- Havnø K, Madsen MN, Dørge J (1995) MIKE 11—a generalized river modelling package. In: Singh VP (ed) *Computer models of watershed hydrology*. Water Resources Publications, Colorado, pp 733–782
- Indu SN, Parimala RS, Elango L (2013) Identification of seawater intrusion by Cl/Br ratio and mitigation through managed aquifer recharge in aquifers North of Chennai, India. *J Groundw Res* 2:155–162
- Kollet SJ, Maxwell RM (2006) Integrated surface-groundwater flow modeling: a free-surface overland flow boundary condition in a parallel groundwater flow model. *Adv Water Resour* 29:945–958
- Kuffour BNO, Engdahl NB, Woodward CS, Condon LE, Kollet S, Maxwell RM (2020) Simulating coupled surface–subsurface flows with ParFlow v3.5.0: capabilities, applications, and ongoing development of an open-source, massively parallel, integrated hydrologic model. *Geosci Model Dev* 13:1373–1397. <https://doi.org/10.5194/gmd-13-1373-2020>
- Kumar P, Lohani AK, Nema AK (2019) Rainfall runoff modeling using Mike 11 Nam Model. *Curr World Environ* 14(1):27–36
- Lafdani EK, Nia AM, Pahlavanravi A, Ahmadi A, Jajarmizadeh M (2013) Daily rainfall–runoff prediction and simulation using ANN, ANFIS and conceptual hydrological MIKE11/NAM Models. *Int J Eng Technol Sci* 1(1):32–50
- Langevin CD, Guo W (2006) MODFLOW/MT3DMS-based simulation of variable-density ground water flow and transport. *Groundwater* 44(3):339–351
- Malamataris D, Kolokytha E, Loukas A (2019) Integrated hydrological modelling of surface water and groundwater under climate change: the case of the Mygdonia basin in Greece. *J Water Clim Change*. <https://doi.org/10.2166/wcc.2019.011>
- Margat J, Gun JVD (2013) *Groundwater around the World: a geographic synopsis*. CRC Press, Balkema
- Markstrom SL, Niswonger RG, Regan RS, Prudic DE, Barlow PM (2008) GSFLOW—coupled ground-water and surface-water flow model based on the integration of the precipitation-runoff modeling system (PRMS) and the modular ground-water flow model

- (MODFLOW-2005). USGS. Chapter 1 of section D, ground-water/surface-water book 6, modeling techniques
- McDonald MG, Harbaugh AW (1988) A modular three-dimensional finite difference ground-water flow model: US geological survey techniques of water-resources investigations, book 6 (chapter A1). US Geological Survey, p 586
- Mishra SK, Pandey RP, Jain MK, Singh VP (2007) A rain duration and modified AMC dependent SCS-CN procedure for long duration rainfall-runoff events. *Water Resour Manag* 22:861–876
- Monninkhoff B (2011) Coupling the groundwater model FEFLOW and the surface water. IfmMIKE11 2.0 user manual. DHI-WASY software
- Monninkhoff B, Hartnack JN (2011) Improvements in the coupling interface between FEFLOW and MIKE11. In: Proceedings of the 2nd international FEFLOW user conference
- Monninkhoff L, Kaden S, Mayer J (2011) Integrated analyses of MAR techniques in Shandong, China. Corpus ID: 221679092
- Mullem JAV (1991) Runoff and peak discharges using green-ampt infiltration model. *J Hydraul Eng* 117:354–370
- Rajaveni SP (2015) Integrated Approach of modelling of runoff, infiltration and density-dependent groundwater flow: a case study in seawater intruded coastal aquifer north of Chennai, India. PhD Thesis, Anna University
- Rajaveni SP, Indu SN, Elango L (2014) Application of remote sensing and GIS techniques for estimation of seasonal groundwater abstraction at Arani–Koratalaiyar river basin, Chennai, Tamil Nadu, India. *Int J Earth Sci Eng* 07(1):248–251
- Rajaveni SP, Indu SN, Elango L (2016) Finite element modelling of a heavily exploited coastal aquifer for assessing the response of groundwater level to the changes in pumping and rainfall variation due to climate change. *Hydrol Res* 47(1):42–60
- Rao SVN, Saheb SM, Ramasastri KS (2004) Aquifer restoration from seawater intrusion: a preliminary field scale study of the Minjur aquifer system, north of Chennai, Tamil Nadu, India. In: 18 Seawater intrusion meeting cartagena, Spain, IGME, pp 707–715
- Sherif MM, Singh VP (1999) Effect of climate change on seawater intrusion in coastal aquifers. *Hydrol Process* 13:1277–1287
- Sivaraman KR, ThillaiGovindaranjan S (2012) A micro level study of A–K basin. The Centre for Science and Environment, New Delhi
- Smits FJC, Hemker CJ (2004) Modelling the interaction of surface-water and groundwater flow by linking DufLOW to MicroFem; FEM_MODFLOW. Czech Republic, Karlovy Vary
- Sophocleous M, Perkins SP (2000) Methodology and application of combined watershed and groundwater model in Kansas. *J Hydrol* 236:185–201
- Suganthi S, Elango L, Subramanian SK (2013) Groundwater potential zonation by remote sensing and GIS techniques and its relation to the groundwater level in the coastal part of the Arani and Koratalai River Basin, Southern India. *Earth Sci Res J* 17(2):87–95
- Swain ED, Wexler EJ (1996) A coupled surface-water and groundwater flow model (MODBRANCH) for simulation of stream-aquifer interaction. Techniques of water-resources investigations of the United States Geological Survey, chapter A6. United States Geological Survey
- Todd DK, Mays LW (2005) Ground-water hydrology, 3rd edn. Wiley, New York, p 636
- Torres-Martinez JA, Mora A, Ramos-Leal JA, Morán-Ramírez J, Arango-Galván C, Mahlknecht J (2019) Constraining a density-dependent flow model with the transient electromagnetic method in a coastal aquifer in Mexico to assess seawater intrusion. *Hydrogeol J*. <https://doi.org/10.1007/s10040-019-02024-w>
- Uhlenbrook S (1999) Prediction uncertainty of conceptual rainfall-runoff models caused by problems in identifying model parameters and structure. *J Hydrol Sci* 44(5):779–797
- UNDP (1987) Hydrogeological and artificial recharge studies, Madras: technical report. United Nations Department of technical co-operation for development, New York
- Vrba J, Gun JVD (2004) The world's groundwater resources. International Groundwater Resources Assessment Centre. http://www.unigrac.org/dynamics/modules/SFIL0100/view.php?fil_Id=126
- Vries JJD (1995) Seasonal expansion and contraction of stream networks in shallow groundwater systems. *J Hydrol* 170:15–26
- Waichler SR, Wigmosta MS (2004) Application of hydrograph shape and channel Infiltration models to an Arid Watershed. *J Hydrol Eng* 9(5):433–439
- Zhang Q, Li L (2009) Development and application of an integrated surface runoff and groundwater flow model for a catchment of Lake Taihu watershed, China. *Quat Int* 208:102–108

Publisher's Note Springer Nature remains neutral with regard to jurisdictional claims in published maps and institutional affiliations.